

~~RESTRICTED~~

UNCLASSIFIED



Inactive

c.2

*Auth. J. W. Crawley 3/25/54
per change 2028 RM No. 4/1/54*

NACA RM No. E8J29

RESEARCH MEMORANDUM

SIMULATED ALTITUDE PERFORMANCE OF COMBUSTOR OF
WESTINGHOUSE 19XB -1 JET-PROPULSION ENGINE

By J. Howard Childs and Richard J. McCafferty

Lewis Flight Propulsion Laboratory
Cleveland, Ohio

CLASSIFICATION CANCELLED

Authority *J. W. Crawley* Date *12/14/53*
EO 10.501

By *AK-1-19-54* See *nada*

CLASSIFIED DOCUMENT *RF 2029*

REVIEWED BUT NOT
EDITED

This document contains classified information affecting the National Defense of the United States within the meaning of the Espionage Act, USC 50c31 and 32. Its transmission or the revelation of its contents in any manner to an unauthorized person is prohibited by law. Information so classified may be imparted only to persons in the military and naval services of the United States, appropriate civilian officers and employees of the Federal Government who have a legitimate interest therein, and to United States citizens of known loyalty and discretion who of necessity must be informed thereof.

NATIONAL ADVISORY COMMITTEE FOR AERONAUTICS

WASHINGTON
November 30, 1948

~~RESTRICTED~~
UNCLASSIFIED

NACA LIBRARY
LEWIS FLIGHT PROPULSION LABORATORY
Langley Field, Va.



UNCLASSIFIED

NATIONAL ADVISORY COMMITTEE FOR AERONAUTICS

RESEARCH MEMORANDUMSIMULATED ALTITUDE PERFORMANCE OF COMBUSTOR OF WESTINGHOUSE 19XB-1
JET-PROPULSION ENGINE

By J. Howard Childs and Richard J. McCafferty

SUMMARY

A 19XB-1 combustor was operated under conditions simulating zero-ram operation of the 19XB-1 turbojet engine at various altitudes and engine speeds. The combustion efficiencies and the altitude operational limits were determined; data were also obtained on the character of the combustion, the pressure drop through the combustor, and the combustor-outlet temperature and velocity profiles.

At altitudes about 10,000 feet below the operational limits, the flames were yellow and steady and the temperature rise through the combustor increased with fuel-air ratio throughout the range of fuel-air ratios investigated. At altitudes near the operational limits, the flames were blue and flickering and the combustor was sluggish in its response to changes in fuel flow. At these high altitudes, the temperature rise through the combustor increased very slowly as the fuel flow was increased and attained a maximum at a fuel-air ratio much leaner than the over-all stoichiometric; further increases in fuel flow resulted in decreased values of combustor temperature rise and increased resonance until a rich-limit blow-out occurred.

The approximate operational ceiling of the engine as determined by the combustor, using AN-F-28, Amendment-3, fuel, was 30,400 feet at a simulated engine speed of 7500 rpm and increased as the engine speed was increased. At an engine speed of 16,000 rpm, the operational ceiling was approximately 48,000 feet. Throughout the range of simulated altitudes and engine speeds investigated, the combustion efficiency increased with increasing engine speed and with decreasing altitude. The combustion efficiency varied from over 99 percent at operating conditions simulating high engine speed and low altitude operation to less than 50 percent at conditions simulating operation at altitudes near the operational limits. The isothermal total-pressure drop through the combustor was 1.82 times as great as the inlet dynamic pressure. As expected from theoretical considerations, a straight-line correlation was obtained when the ratio of the combustor total-pressure drop to the combustor-inlet dynamic pressure was plotted as a function of the ratio of the combustor-inlet air

~~RESTRICTED~~

UNCLASSIFIED

density to the combustor-outlet gas density. The combustor-outlet temperature profiles were, in general, more uniform for runs in which the temperature rise was low and the combustion efficiency was high. Inspection of the combustor basket after 36 hours of operation showed very little deterioration and no appreciable carbon deposits.

INTRODUCTION

Performance studies of 19XB-1 turbojet engine conducted in the Cleveland altitude wind tunnel (reference 1) indicated that the engine operated satisfactorily at low altitudes, but as the simulated altitude was increased at any given rotational speed, engine operation first became sluggish and then failed at a certain altitude. The engine operational failures were characterized by a decrease of turbine speed and the appearance of long flames extending from the engine exhaust nozzle; increasing the fuel flow resulted in further deceleration of the engine and longer exhaust flames until combustion ceased.

Similar operation, but with lower limiting altitudes than those found with the 19XB-1, was obtained in a wind-tunnel investigation on the 19B engine (reference 1). An investigation was made of the performance of the combustor in the combustion laboratory and it was shown that the altitude operational limits of the 19B engine are imposed by the combustor (reference 2); the 19XB-1 engine uses the same combustor as the 19B engine. Reference 2 also reported that performance of the 19B combustor was adversely affected by decreasing the inlet-air pressure or temperature and by increasing the inlet-air velocity. The higher compression ratio of the 19XB-1 compressor therefore results in conditions of the combustor-inlet air in the 19XB-1 engine more favorable to the combustion process and hence a higher altitude operational limit would be expected.

The altitude performance of the 19XB-1 combustor was investigated at the NACA Cleveland laboratory under conditions simulating zero-ram operation of the 19XB-1 engine at various altitudes and rotational speeds. This investigation was conducted during the period December 1945 to March 1946. The altitude operational limits and combustion efficiencies in the operational range are presented. The altitude operational limits were indicated by failure of the combustor to supply the combustor-outlet temperature required for operation of the engine. Data were also obtained on the character and appearance of the combustion, the general condition of the combustor, the total-pressure drop through the combustor, and the combustor-outlet temperature and velocity profiles.

APPARATUS AND INSTRUMENTATION

Combustor

A diagrammatic cross section of the combustor installation is shown in figure 1. The combustor in the 19XB-1 engine, which is the same as the 19B combustor, is approximately 19 inches in diameter and fills the annular space around the compressor-turbine shaft of a 19XB-1 turbojet engine. A description of the combustor is given in reference 2.

Apparatus

A diagram of the general arrangement of the installation is shown in figure 2. The combustor was connected to the laboratory air supply and exhaust systems and the air quantities and pressures were regulated by remote-control valves. The exhaust gases were cooled by means of water sprays in the vertical exit pipe.

For regulation of inlet-air temperatures, a portion of the air was burned with gasoline in a preheater and then mixed uniformly with the rest of the air upstream of the combustor. The preheater was operated at conditions giving efficient combustion in order to minimize contamination of the air by combustibles. The use of such a preheater to produce a 200° F rise in the inlet-air temperature results in a consumption of 3.9 percent of the oxygen, an increase in the carbon-dioxide content of the inlet air by 0.80 percent of the total air weight, and an increase in the moisture content by 0.36 percent of the total air weight.

The inlet and outlet ducts were fabricated to simulate the dimensions and contours of the engine ducts leading to and from the combustor. Figure 1 shows the longitudinal cross section of the combustor and adjacent ducting and indicates the location of instrumentation planes. Observation windows for viewing the combustion were provided in the combustor housing as shown in figures 2 and 3. Another observation window, located in the vertical exit pipe (fig. 2), provided an end view of the inside of the combustor.

Temperature and velocity profiles at the combustor inlet were made uniform by first introducing turbulence to mix the air thoroughly with the exhaust gas from the preheater and then removing the turbulence in a calming chamber. (See fig. 2.) Maximum differences between local inlet temperatures and the mean temperature were about 5° F and occurred only in runs with high preheat temperatures.

The maximum and minimum inlet velocities deviated by about 5 percent from the mean velocity for most runs. The 24 fuel nozzles in the combustor were periodically calibrated and replaced when necessary; these nozzles were well matched, having maximum deviations of ± 3 percent from the mean fuel delivery when individually calibrated at a pressure differential of 25 pounds per square inch.

Instrumentation

The thermocouple junctions and the pressure taps in each instrumentation plane were located at centers of equal areas, as shown in figure 4. The letter positions at all instrumentation planes are arranged clockwise as seen looking upstream. A tabulation of the number and type of instruments at each plane follows:

Instruments	Instrumentation plane					
	2			3		
	Number of rakes	Probes per rake	Total number of probes	Number of rakes	Probes per rake	Total number of probes
Thermocouples	8	1	8	16	3	48
Total-pressure tubes	4	4	16	8	4	32
Wall-static pressure orifices			5			4

Instrumentation plane 2 (fig. 1) is located at the combustor inlet, which has a cross-sectional area of 0.647 square foot; instrumentation plane 3 (fig. 1) is at the combustor outlet where the annular cross-sectional area is 0.858 square foot. The pressure taps at plane 3 were located 1 inch downstream of the thermocouple rakes. Construction details of the temperature- and pressure-measuring instruments are shown in figure 5.

Pressure data were obtained from photographs of manometers. The thermocouples were connected through multiple switches to two calibrated, self-balancing potentiometers, one with -100° to 700° F range to record the inlet temperatures and one with 400° to 2400° F range to record the outlet temperatures. Fuel flows to the combustor and preheater were metered separately with calibrated rotameters. The pressure differential across the fuel nozzles was measured when possible by a 50-inch mercury manometer; higher pressure differentials were determined by obtaining the fuel manifold pressure with a Bourdon-type gage and correcting for the combustor-inlet pressure. The air flow to the combustor was metered by a square-edge orifice installed according to A.S.M.E. specifications and located upstream of all regulating valves.

PROCEDURE

Program

The program was divided into two principal investigations: (a) determination of altitude operational limits, and (b) determination of combustor efficiencies. Estimated combustor-inlet conditions and combustor-outlet temperatures corresponding to zero-ram operation for the 19XB-1 engine at various altitudes and engine speeds were supplied by the manufacturer and are shown in figure 6. These data were used to set the combustor operating conditions necessary to simulate engine operation at any desired altitude and engine speed.

In order to determine the altitude operational limits, the combustor was operated with inlet conditions of air flow, pressure, and temperature simulating engine operation at various altitudes and engine speeds. For each simulated altitude - engine-speed condition the fuel flow (AN-F-28, Amendment-3, fuel) was varied through a wide range in an attempt to obtain the combustor-outlet temperature required for nonaccelerating engine operation. If the required combustor-outlet temperature could be obtained, the simulated altitude and engine speed was considered within the operational range of the engine; if the required combustor-outlet temperature was unobtainable, the *simulated* altitude and engine speed was considered within the nonoperational range of the engine. In order to obtain general combustor performance information, data were usually recorded and the combustion characteristics noted as each of the following events occurred: (1) An average combustor-outlet temperature was obtained that was equal to or slightly above the nonaccelerating engine requirement; (2) the character of the

combustion changed; (3) maximum obtainable (peak) value of average combustor-outlet temperature was reached; (4) some local outlet temperatures exceeded the potentiometer limit (2400° F) and were considered unsafe for the instrumentation, making a further increase in fuel flow inadvisable; and (5) combustion ceased (blow-out). The sequence and the number of these events varied for different points.

The combustor was operated over a more extensive range of altitudes and engine speeds than necessary to determine altitude operational limits to obtain combustion efficiencies. For each altitude - engine-speed condition selected for study, the air flow and the pressure and temperature at the combustor inlet were maintained constant at the values shown in figure 6 and the fuel flow (AN-F-28 fuel) was altered to give an average outlet temperature approximately equal to that required for nonaccelerating engine operation (fig. 6(d)). The average combustor-outlet temperature was difficult to estimate because the outlet-temperature distribution was nonuniform; data were therefore usually recorded at two or more fuel flows that gave average combustor-outlet temperatures slightly above and slightly below the required value. An interpolation was then made between the combustion efficiencies for these outlet temperatures to obtain the combustion efficiency for an average combustor-outlet temperature equal to the nonaccelerating engine requirement.

Methods of Calculation

The average dynamic pressures at instrumentation planes 2 and 3 were computed from the air flow, the fuel flow, and the average temperatures and static pressures measured at these instrumentation planes. The total-pressure drop across the combustor was obtained as follows: Static pressures at instrumentation planes 2 and 3 were measured, the average dynamic pressures were added to these values to give total pressures at the combustor inlet and outlet, and the difference between these values was taken as the total-pressure drop across the combustor.

In order to determine velocity profiles, the local velocities at several points were computed from the measured values of total pressure and temperature at those points together with the average static pressure at that cross section.

The combustion efficiency is arbitrarily defined as the ratio of the actual rise in total temperature to the theoretical rise in total temperature possible with the fuel-air ratio used. The charts

of reference 3 were utilized for these computations. The thermocouple indications were taken as true values of the total temperatures with no corrections being made for radiation or stagnation effects.

RESULTS AND DISCUSSION

Altitude Operational Limits

Experimentally determined data obtained to ascertain altitude operational limits are summarized in table I. Data on combustor-outlet conditions are omitted from table I for runs in which any of the following events occurred: (1) Several individual readings of combustor-outlet temperatures fell below the potentiometer limit (400° F) making it impossible to determine accurately the average combustor-outlet temperature; (2) large fluctuations occurred in the instrument indications; (3) blow-out occurred when the fuel-air ratio was changed to the value indicated; and (4) no combustion was obtainable at any fuel-air ratio. The runs for which data are omitted are labeled in table I to indicate which of these phenomena was the cause.

The altitude operational limits are presented in figure 7 on a plot of the simulated altitudes and engine speeds. The curve separates the region where the combustor-outlet temperatures obtainable were sufficient from the region where the outlet temperatures obtainable were insufficient for nonaccelerating operation of the 19XB-1 engine. For convenience in referring to table I, the data points on the figure are identified by numbers. The approximate operational ceiling of the engine as determined by the combustor was 30,400 feet at a simulated engine speed of 7500 rpm and increased as the simulated engine speed was increased. At an engine speed of 16,000 rpm, the operational ceiling of the engine was approximately 48,000 feet.

No runs were made at conditions simulating flight velocities other than zero, but it is estimated from the data reported here and in reference 2 that the altitude operational limits will be at least 5000 feet higher throughout the entire engine-speed range when a flight velocity of 500 miles per hour is simulated.

A comparison is made in figure 8 of the altitude operational limits of the combustor determined herein with (a) the operational limits obtained in an altitude-wind-tunnel investigation of the 19XB-1 engine at a simulated flight velocity of 200 miles per hour and

using AN-F-22 fuel (reference 1), and (b) the operational limits obtained with this same combustor at 19B engine zero-ram conditions and using AN-F-28 fuel (reference 2). The first comparison shows the results of the combustor investigation to be in fair agreement with the results of the engine investigation. The curve determined by the engine investigation would be expected to be higher than the curve determined by the combustor investigation because 200 miles per hour ram was used with the engine. Comparison (b) shows the benefit to the combustor of changing to a higher compression-ratio compressor, which is the main difference between the 19B and the 19XB-1 turbojet engines. The sensitivity of the combustor to the compressor performance is accounted for by data presented in reference 2 showing the effects of inlet-air pressure, temperature, and velocity on combustor performance.

Combustion Efficiencies

Results of the combustion-efficiency investigation are summarized in table II. Lines of constant combustion efficiency (dashed lines) are shown on a plot of simulated altitudes and engine speeds in figure 9. At each data point on the figure, the combustion efficiency for that point is specified. The constant combustion-efficiency lines were obtained by interpolating between the data points. The solid curve on figure 9 represents the altitude operational limits as determined herein. Throughout the range of simulated altitudes and engine speeds investigated, the combustion efficiency increased with increasing engine speed and with decreasing altitude. For example, at an altitude of 20,000 feet the combustion efficiency was 64 percent at 7000 rpm, 76 percent at 10,000 rpm, and 98 percent at 14,000 rpm; at sea level the combustion efficiency was 93 percent at 7000 rpm and 99 percent at 10,000 rpm. Combustion efficiencies below 50 percent were obtained at altitudes near the operational limits.

Available Acceleration

The amount by which the combustor temperature rise obtainable exceeds the temperature rise required for nonaccelerating engine operation is an index of the available acceleration. For many simulated altitudes and engine speeds, data showing the maximum temperature rise obtainable appear in table I. The differences between these maximum values of temperature rise obtainable and the corresponding values of temperature rise required for nonaccelerating engine operation at the same altitude and engine-speed conditions

are indicated in figure 10 beside each data point. The data points are located in figure 10 by the coordinates of simulated altitudes and simulated engine speeds and the dashed lines indicate constant values of available acceleration (indicated by the parameter, temperature rise obtainable minus temperature rise required) obtained by interpolating between the data points. The solid curve in figure 10 represents the altitude operational limits and is therefore a curve of zero available acceleration.

Combustion Characteristics

Various types of resonant combustion were observed during the investigations. The resonance was characterized by flickering of the flames, vibration of the combustor and adjacent ducting, and fluctuation of the outlet-temperature indications. The combustion during each run is described by a letter designation in tables I and II.

For any simulated engine speed at altitudes to within about 10,000 feet of the operational limit, nonresonant yellow-flame combustion occurred and the combustor supplied a temperature rise far in excess of that required for engine operation; the combustor temperature rise increased with fuel-air ratio throughout the range of fuel-air ratios investigated. As the simulated altitude was increased at any constant simulated engine speed, blue-flame combustion gradually appeared and then resonance appeared and became pronounced as the operational limit was approached. At altitudes near the operational limit, the combustor showed little response to changes in fuel flow. The temperature rise through the combustor increased very slowly as the fuel flow was increased and reached a maximum at a fuel-air ratio within the range investigated (much leaner than the over-all stoichiometric); further increases in fuel flow resulted in decreasing combustor temperature rise and increasing resonance until a rich-limit blow-out occurred. At simulated engine speeds below 8000 rpm and at simulated altitudes near the operational limits, combustion would sometimes cease as the fuel flow was decreased (lean-limit blow-out). This phenomenon was never encountered at high simulated engine speeds.

Pressure Drop through Combustor

The data for the total-pressure drop from the inlet to the outlet of the combustor are presented in figure 11. All data from table I are included on the figure. The ratio of the total-pressure

drop to the inlet dynamic pressure $\frac{\Delta P(2-3)}{q_2}$ is plotted against the ratio of the inlet-air density to the outlet-gas density ρ_2/ρ_3 . A straight line with a slope of approximately 0.4 is obtained that represents the data with a scatter of about ± 5 percent. A derivation of this relation is presented in reference 2 where it is explained that the relation does not hold accurately for this combustor when the flame seat shifts. The flame seat was observed to move farther downstream when operating under conditions that result in resonant combustion or when operating with a high heat release (high air-flow rate together with high combustor-temperature rise).

The same pressure-drop data are expressed in figure 12 as a function of the ratio of combustor-outlet temperature to combustor-inlet temperature T_3/T_2 . Figure 12 makes possible the direct estimation of the pressure drop across the combustor from a knowledge of compressor and turbine performance although the correlation is less exact theoretically than that of figure 11.

The isothermal $\frac{\Delta P(2-3)}{q_2}$ is 1.82. When T_3/T_2 is 2.6, $\frac{\Delta P(2-3)}{q_2}$ is about 2.5. These values of pressure drop across the combustor are about 14 percent higher than those reported in reference 2 for the same combustor. The high values for the pressure drop reported may result because the pressure taps at instrumentation plane 3 were located a short distance downstream of the thermocouple rakes and recorded the additional pressure drop across those rakes; this condition was not present in reference 2.

Temperature and Velocity Profiles at Combustor Outlet

Combustor-outlet temperature profiles became more uniform (1) as the average combustor-temperature rise decreased and (2) as the inlet conditions were altered to give higher combustion efficiency. These general trends were consistent although the exact pattern of an outlet-temperature distribution could not always be reproduced in check runs. In order to illustrate these trends, combustor-outlet temperature profiles for 3 runs are presented in figure 13. A comparison of the pertinent data for the three runs follows:

	Average combustor-temperature rise (°F)	Combustion efficiency (percent)	Average combustor-outlet temperature (°F)	Maximum local outlet temperature (°F)	Minimum local outlet temperature (°F)	Average outlet-temperature deviation (°F)
Run shown in fig. 13(a) (10,000 rpm at 15,000 ft)	713	86.8	834	1160	585	94.8
Run shown in fig. 13(b), (10,000 rpm at 10,000 ft)	713	90.8	853	1070	630	84.2
Run shown in fig. 13(c), (17,000 rpm at 47,000 ft)	1218	86.5	1459	1970	970	150.6

The average outlet-temperature deviation is the average deviation of the individual local temperatures from the average temperature at the combustor outlet.

A comparison was made between the combustor-outlet temperature profiles for two runs (figs. 13(a) and 13(b)) in which the combustor-temperature rise was the same but the combustion efficiency was different; the run shown in figure 13(a) had the lower combustion efficiency and the more uneven outlet-temperature profile. Figures 13(a) and 13(c) afford a comparison between the combustor-outlet temperature profiles for two runs in which the combustion efficiency was about the same but the combustor-temperature rise was different; the run shown in figure 13(c) had the higher temperature rise and the more uneven outlet-temperature profile. The temperature profiles at the combustor outlet were very sensitive to alinement of the combustor basket.

Figure 14 shows combustor-outlet velocity profiles for the same runs for which combustor-outlet temperature profiles appear in figure 13. The velocity profiles were similar for all runs and their degree of uniformity showed no direct relation to the temperature profiles.

Condition of Combustor Basket

Inspection of the basket at the conclusion of the investigation to determine the altitude operational limits (about 16 hr running time) showed very little warping and only slight carbon deposits (at the upstream end of the basket). At the conclusion of the investigation to determine combustion efficiencies (about 20 hr operation), the basket showed very little warping and the carbon deposits, though considerably greater than those formed during the altitude-operational-limits investigation, were still less than 0.003 inch thick at the upstream end of the basket. Most of the carbon deposited was in the form of soot. The carbon deposits formed during the efficiency investigation were greater than those formed during the operational-limits investigation and may be the result of the prolonged operation at low simulated altitudes where yellow, luminous flames are encountered. The inside surface of the basket was covered by deposits of lead oxide. These deposits were also amorphous in nature and were never thicker than the carbon deposits at the upstream end of the basket.

SUMMARY OF RESULTS

The results obtained in the investigation of the combustor for the 19XB-1 turbojet engine at conditions simulating zero-ram operation at various altitudes and rotational speeds are summarized as follows:

1. For any simulated engine speed at all altitudes to within about 10,000 feet of the operational limit, yellow-flame combustion occurred and the combustor supplied a temperature rise far in excess of that required for engine operation; the combustor temperature rise increased with fuel-air ratio throughout the range of fuel-air ratios investigated.

2. As the simulated altitude was increased, at any constant simulated engine speed, blue-flame combustion gradually appeared and then resonance appeared and became pronounced as the operational limit was closely approached. At altitudes near the operational limit, the response of the combustor to changes in fuel flow was very slow. The temperature rise through the combustor increased slowly as the fuel flow was increased and attained a maximum value at a fuel-air ratio within the range investigated (much leaner than the over-all stoichiometric); further increases in fuel flow resulted in decreasing temperature rise and increasing resonance until a rich-limit blow-out occurred.

3. The operational ceiling of the engine, as indicated by failure of the combustor to supply the energy required by the turbine, was 30,400 feet at a simulated engine speed of 7500 rpm and the operational ceiling increased as the simulated engine speed was increased.

4. The altitude operational limits, which were imposed on the 19B engine by the combustor, were much lower than those imposed on the 19XB-1 engine. This difference was due to the more favorable combustor-inlet conditions obtained with the higher compression ratio in the 19XB-1 engine.

5. Throughout the range investigated, the combustion efficiency increased with increasing engine speed and with decreasing altitude. At an altitude of 20,000 feet the combustion efficiencies were 64 percent at 7000 rpm, 76 percent at 10,000 rpm, and 98 percent at 14,000 rpm. At sea level, the combustion efficiencies were 93 percent at 7000 rpm and 99 percent at 10,000 rpm. Combustion efficiencies below 50 percent were obtained at altitudes near the operational limits.

6. As expected from theoretical considerations, a straight-line correlation was obtained when the ratio of the total-pressure drop through the combustor to the combustor-inlet dynamic pressure was plotted as a function of the ratio of the combustor-inlet air density to the combustor-outlet gas density. The isothermal total-pressure drop through the combustor was 1.82 times as great as the inlet-dynamic pressure.

7. Combustor-outlet temperature profiles were more uniform when the temperature rise through the combustor was low and when the combustion efficiency was high.

8. Inspection of the combustor basket showed little deterioration and no appreciable carbon deposits after 36 hours of operation.

Lewis Flight Propulsion Laboratory,
National Advisory Committee for Aeronautics,
Cleveland, Ohio

REFERENCES

1. Fleming, William A.: Altitude-Wind-Tunnel Investigation of Westinghouse 19B-2, 19B-8, and 19XB-1 Jet-Propulsion Engines. I - Operational Characteristics. NACA RM No. ESJ28, 1948.
2. Childs, J. Howard, McCafferty, Richard J., and Surine, Oakley W.: Effect of Combustor-Inlet Conditions on Performance of an Annular Turbojet Combustor. NACA TN No. 1357, 1947.
3. Turner, L. Richard, and Lord, Albert M.: Thermodynamic Charts for the Computation of Combustion and Mixture Temperatures at Constant Pressure. NACA TN No. 1086, 1946.

1 1

1 1

1 1

•

•

•

TABLE I - PERFORMANCE DATA ON COMBUSTOR OF 19XB-1 TURBOJET

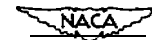
Point	Simulated engine speed (rpm)	Simulated altitude (ft)	Inlet static pressure (lb/sq in. absolute)	Inlet-air total temperature (°F)	Average outlet total temperature (°F)	Average total temperature rise through combustor (°F)	Air flow (lb/sec)	Fuel flow (lb/hr)	Fuel-air ratio	Combustion efficiency
1	6,000	2,000	5.35	-4	---	---	2.70	200-500	---	---
2	6,000	7,000	5.79	0	870	570	2.85	222	0.0214	0.583
			5.79	0	908	908	2.85	340	.0328	.424
			5.79	0	---	---	2.	372	.0360	---
4	10,000	18,000	9.82	75	886	791	6.29	402	0.0177	0.658
			9.82	75	954	879	6.29	488	.0205	.620
			9.82	76	998	923	6.29	500	.0220	.612
			9.82	76	1142	1067	6.29	500	.0220	.707
			9.82	76	958	865	6.29	600	.0264	.488
5	10,000	2,000	8.30	60	623	623	5.38	300	0.0177	0.528
			8.30	61	656	656	5.38	300	.0198	.432
			8.30	60	653	593	5.38	385	---	---
7	14,000	16,000	12.27	150	1300	1363	7.30	7,700	0.0264	0.779
12	14,000	10,000	10.21	150	1248	1098	6.06	466	0.0208	0.770
			10.21	150	1398	1248	6.04	550	.0252	.740
			10.21	150	---	---	6.04	600	.0275	---
31	14,000	14,000	8.54	150	947	797	6.06	412	0.0191	0.604
			8.54	150	1024	274	6.05	415	.0226	.572
			8.54	151	916	765	5.09	509	.0226	.500
			8.54	150	955	805	5.06	525	.0288	.428
32	14,000	18,000	7.02	150	668	516	4.19	300	0.0197	0.582
			7.02	151	618	667	4.19	425	.0280	.565
			7.02	---	---	---	4.19	520	.0344	---
34	10,000	15,000	7.37	1	---	---	4.82	303	0.0173	---
			7.37	51	534	534	4.82	345	.0197	0.390
			7.37	128	---	---	4.82	380	.0218	---
36	8,000	50,000	6.97	24	697	661	4.10	300	0.0201	0.477
			6.97	---	685	---	4.10	340	.0228	.421
37	8,000	32,000	0.38	15	630	615	3.77	350	0.0241	0.385
			---	25	---	---	3.85	345	.0249	---
38	10,000	50,000	9.03	70	685	665	5.77	300	0.0144	0.871
			9.03	69	798	798	5.78	370	.0176	.644
			9.03	70	822	822	5.77	425	.0204	.583
			9.03	70	823	823	5.77	464	.0223	.540
			9.03	69	---	---	5.77	520	.0250	---

¹The following types of resonant combustion were encountered:

- A Rapid flickering at base of flame.
- B Temperature fluctuations at combustor outlet.
- D Noisy vibration of combustor and adjacent ducting together with temperature fluctuations at combustor outlet.
- E Rapid flickering at base of flame together with temperature fluctuations at combustor outlet.
- N Normal operation (no noticeable resonance).
- + severe intensity.
- Slight intensity.

²The following conditions made some data unobtainable:

- W Blow-out.
- X Fluctuations in outlet temperatures.
- Y outlet temperatures below 400° F.
- Z No combustion at any fuel-air ratio.



ENGINE FROM TESTS TO DETERMINE ALTITUDE OPERATIONAL LIMITS

Point	Maximum local outlet total temperature (°F)	Minimum local outlet total temperature (°F)	Total-pressure drop (lb/sq in.)	Static-pressure drop (lb/sq in.)	Pressure difference across fuel nozzles (in. Hg)	Inlet velocity (ft/sec)	Average outlet velocity (ft/sec)	Remarks (1),(2)
1						131		Z
2	1200 1620	400 550	.166	0.22	5.4 9.8 12.0	129 129 129	311	E E+ E+, W
4	1180 1340 1610 1600 1500	610 680 710 700 600	0.49 .50 .52 .58	0.64 .67 .76	14.3 18.3 22.8 23.1 34.3	195 196 195 195 195	396 426 440 489	N A- D- D D
5	850 930 860	450 440 480	0.39 .51 .39	0.44 .44 .44	8.0 9.8 11.8	192 192 192	324 331 334	E- E E+
7	1700 1990	910 1050	0.68 .73	0.88 1.01	25.1 45.9	207 207	494 564	D- D
12	1740 1870	870 980	0.54 .60	0.70 .80	17.1 28.0	206 206 206	477 526	N B D+, X
31	1400 1450 1200 1230	720 710 670 760	0.44 .44 .41	0.52 .53 .49	11.0 15.4 14.7 26.4	206 206 208 206	388 411 383	D- B A E+
32	1190 1140	400 570	0.31 .32	0.33 .37	8.6 16.4	208 208 208	309 356	E E+ E+, W
34	760	400	0.31	0.35	7.2 10.2	190 190 190	299	E-, Y E E+, W
36	1060 940	510 520	0.28 .25	0.33 .31	9.0 10.4	163 162	313 310	A- E
37	900	430	0.20	0.28	9.6 9.4	160 170	300	E+ A+, W
38	880 1130 1060 1070	540 590 630 630	0.42 .42 .44 .45	0.48 .51 .53 .54	7.8 12.8 15.8 18.8	193 193 193 193 193	337 373 382 384	N A- A E E+, W



TABLE I - PERFORMANCE DATA ON COMBUSTOR OF 19XB-1 TURBOJET

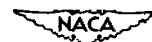
Point	Simulated engine speed (rpm)	Simulated altitude (ft)	Inlet static pressure (lb/sq in. absolute)	Inlet air total temperature (°F)	Average outlet total temperature (°F)	Average total temperature rise through combustor (°F)	Air flow (lb/sec)	Fuel flow (lb/hr)	Fuel-air ratio	Combustion efficiency
39	8,000	28,000	7.71	36	- A - -	-----	4.41	230	0.0144	-----
			7.71	35	817	817	4.41	358	.0224	0.550
			7.71	35	858	858	4.41	410	.0257	.494
			7.71	35	t - - -	I I - -	4.41	460	.0289	-----
40	12,000	35,000	9.97	98	818	720	6.29	320	0.0140	0.721
41	12,000	40,000	9.97	97	1240	1145	6.28	497	.0220	.761
			7.91	98	711	613	4.96	300	0.0166	0.523
			7.91	96	-----	-----	5.04	375	.0207	-----
			7.91	98	754	656	4.95	400	.0223	.430
42	12,000	42,000	7.27	98	600	502	4.58	300	0.0180	0.400
			7.27	98	629	551	4.58	325	.0225	.392
			7.27	98	604	506	4.58	370	.0254	.532, 532
			7.27	98	-----	-----	4.58	420	.0254	-----
43	16,000	50,000	7.91	211	1055	844	4.30	350	0.0224	0.558
			7.91	210	1047	837	4.30	400	.0257	.492
			7.91	210	971	751	4.30	475	.0306	.386
			7.91	210	-----	-----	4.30	500	.0323	-----
44	16,000	47,000	9.43	210	1398	1188	4.95	400	0.0223	0.788
			9.43	210	1397	1187	4.95	450	.0282	.710
46	11,000	38,000	7.51	74	573	499	4.93	375	0.0211	0.348
			7.51	74	-----	-----	4.93	410	.0231	-----
47	14,000	16,000	7.66	152	675	523	4.71	370	0.0218	0.353
			7.68	152	-----	-----	4.71	405	.0239	-----
48	11,000	36,000	8.20	71	613	542	5.40	315	0.0162	0.472
			8.20	87	558	491	5.39	345	.0178	.393
			8.20	71	-----	-----	5.40	420	.0216	-----
49	10,000	58,000	8.08	58	557	499	5.29	325	0.0171	0.414
			8.06	58	547	489	5.29	375	.0197	.357

¹The following types of resonant combustion were encountered:

- A Rapid flickering at base of flame.
- B Temperature fluctuations at combustor outlet.
- D Noisy vibration of combustor and adjacent ducting together with temperature fluctuations at combustor outlet.
- E Rapid flickering at base of flame together with temperature fluctuations at combustor outlet.
- + Severe intensity.
- Slight intensity.

²The following conditions made some data unobtainable:

- W Blow-out.
- x Fluctuations in outlet temperatures.
- Y Outlet temperatures below 400° F.
- Z No combustion at any fuel-air ratio.



ENGINE FROM TESTS TO DETERMINE ALTITUDE OPERATIONAL LIMITS. - Concluded

oint	Maximum local outlet total temperature (°F)	Minimum local outlet total temperature (°F)	Total-pressure drop (lb/sq in.)	Static-pressure drop (lb/sq in.)	Pressure differential across fuel nozzles (in. Hg)	Inlet velocity (ft/sec)	Average outlet velocity (ft/sec)	Remarks (1), (2)
39	1120	590	0.28	0.35	4.8	162	336	E-, Y
	1200	590	.29	.37	12.0	162	349	A-
			-		15.2	162		E+, W
40	1060	640	0.53	0.62	8.8	201	375	N
	1900	640	.58	.78	28.0	200	510	D
41	990	520	0.40	0.45	9.4	199	340	E
					12.1	202		A+, W
	980	560	.40	.46	14.8	199	354	E+
	1000	470	.40	.47	18.0	202	364	A+
42	910	400	0.36	0.39	8.6	200	309	A
	1040	400	"	.39	10.0	200	318	A
	840	400	.35	.38	12.4	200	311	A
						200		E+, W
43	1620	530	0.34	0.40	13.2	208	381	A-
	1480	760	.35	.41	15.0	208	381	A+
	1260	700	.33	.38	21.6	208	362	A+
						208		A+, W
44	2040	890	0.44	0.56	18.0	200	456	N
	2170	890	.41	.53	21.4	200	455	E
46	780	400	0.37	0.41	11.9	200	315	A+
						200		A+, W
47	910	400	0.38	0.40		215	324	A+
						215		A+, W
48	840	400	0.42	0.46	10.5	199	527	N
	830	400			11.5	198		A
					15.1	199		A+, W
49	900	400	0.37	0.41	9.5	194	308	A-
	790	400	.38	.41	11.5	194	306	A



TABLE XI - PERFORMANCE DATA ON COMBUSTOR OF 19XB-1 TURBOJET ENGINE

Point	Simu- lated engine speed (rpm)	Simu- late% alti- tude (ft)	Inlet static pressure (lb/sq in. absolute)	Inlet- air total tempera- ture (°F)	Average outlet total temper- ature (°F)	Aver age total temper- ature rise through combus- tor (°F)	Air flow (lb/ sec)	Fuel flow a (lb/ hr)	Fuel- i r ratio	combus- 'tion effi- ciency
so	7,000	25,000	8.20	32	668	636	4.12	243	0.0164	0.544
---	---	---	9.53	29	836	807	4.12	277	.0187	.613
51	7,000	20,000	---	49	861	812	4.94	297	.0167	.687
---	---	---	9.63	50	701	651	4.94	272	.0153	.597
52	7,000	15,000	11.69	66	812	746	5.74	277	.0134	.773
---	---	---	11.69	66	880	814	6.76	302	.0146	.781
53	7,000	10,000	14.09	81	956	743	6.75	307	.0126	.816
---	---	---	14.09	83	945	a73	6.80	352	.0144	.849
54	7,000	5,000	16.84	101	844	844	7.91	377	.0132	.891
---	---	---	16.84	101	836	735	7.91	337	.0118	.860
55	10,000	20,000	13.40	104	808	704	0.00	354	.0123	.791
---	---	---	13.40	104	690	586	8.00	317	.0110	.730
56	10,000	16,000	15.96	122	793	671	9.50	367	.0107	.858
---	---	---	16.96	121	834	713	9.32	388	.0113	.868
57	---	---	---	---	---	---	---	---	---	---
58	10,000	10,000 5,000	19.20 22.73	158 140	853 918	713 760	12.69 10.90	423 512	.0112	.942
59	14,000	30,000	15.61	170	979	809	9.18	418	.0126	.899
---	---	---	15.61	168	914	746	9.18	388	.0117	.888
60	14,000	25,000	18.95	186	876	690	11.00	416	.0105	.908
---	---	---	18.95	186	938	752	11.00	448	.0113	.926
m - m -	---	---	18.95	186	978	792	10.92	466	.0119	.931
61	14,000	20,000	22.83	207	987	780	13.01	522	.0111	.977
63	17,000	47,000	10.51	241	1355	1114	5.39	372	.0192	.851
---	---	---	10.51	241	1459	1218	5.41	405	.0208	.865
64	17,000	40,000	14.29	240	1347	1107	7.35	469	.0177	.912
---	---	---	14.29	243	1406	1246	7.35	519	.0196	.937
65	17,000	35,000	18.02	243	1444	1201	9.18	598	.0181	.969
---	---	---	18.02	243	1335	1092	9.18	539	.0163	.970
66	17,000	30,000	22.00	279	1367	1088	11.20	637	.0158	.998
69	7,000	---	19.93	119	1025	906	9.09	443	.0135	.940
---	---	---	19.93	119	923	804	9.09	398	.0122	.913
70	10,000	---	26.81	176	963	787	14.46	571	.0110	.994

¹ The following types of combustion were encountered:

- F Rapid flickering at base of flame together with temperature fluctuations at combustor outlet.
- N Normal operation (no notlaeable resonance).
- Slight intensity.



FROM TESTS TO DETERMINE ALTITUDE COMBUSTION EFFICIENCIES

Point	Maximum local outlet total temperature (°F)	Minimum local outlet total temperature (°F)	Total pressure drop (lb/sq in.)	Static pressure drop (lb/sq in.)	Pressure differential across fuel nozzles (in. Hg)	Inlet velocity (ft/sec)	Average outlet velocity (ft/sec)	Remark (1)
50	850	460	0.226	0.264	8.0	141	256	E
51	1080	530	.240	.300	8.6	140	296	E
51	1240	530	.299	.372	7.0	151	311	N
52	910	460	.278	.325	7.2	161	272	E
52	1220		.314	.379		147		N
		500					281	N
53	1130	560	.363	.433	8.0	248	298	N
54	1270 1360	700 670	.382	.480	10.8	149	308	N
				.531	12.8			N
		620				150	297	N
55	1180	560	.536	.632	9.0	150	298	N
56	1000	450	.621	.581	12.2	192	312	N
56	1000	580	.640	.736		198	352	N
58	1160	585	.694	.754	13.7	198	338	N
59	1070	740 740	.872	.809	16.7	194		N
				.996			350	N
	1290			.801	15.8	211	388	N
	1200	670	.664	.773	23.6	211	370	N
60	1080	660	.776	.977	16.2	214	353	N
	1170	730	.764	.888	20.9	214	370	N
61	1210	750	.777	.917	27.2	212	379	N
63	1190	800	.947	1.097		217	376	N
	1850	960		.578	15.2	205	432	E
	1970	970	.489	.602	16.4	206	460	N
64	1830	980	.590	.740	20.8	205	429	N
	2000	1070	.606	.791	26.2	205	464	N
65	1890	1130		.924	37.2		448	N
66			.712			204		N
69	1600	1790	.479	1.051	22.5	204	429	N
	1300			.603	18.8	150	304	N
	1160	720	.471	.570	14.8	150	283	N
70	1200	780	.942	1.108	33.3	195	348	N



694

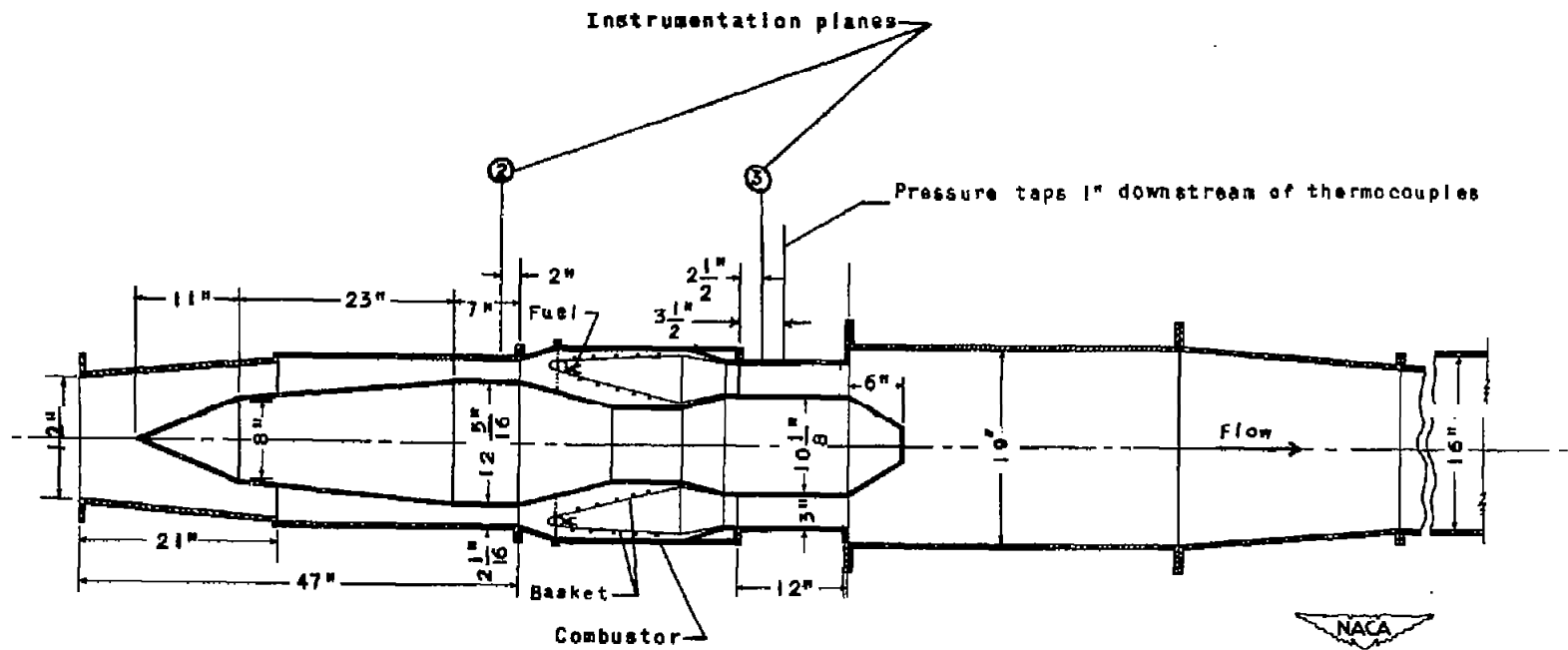


Figure 1. - Diagrammatic sketch of installation of combustor for 19XB-1 turbojet engine showing inlet and outlet ducts and locations of instrumentation planes.

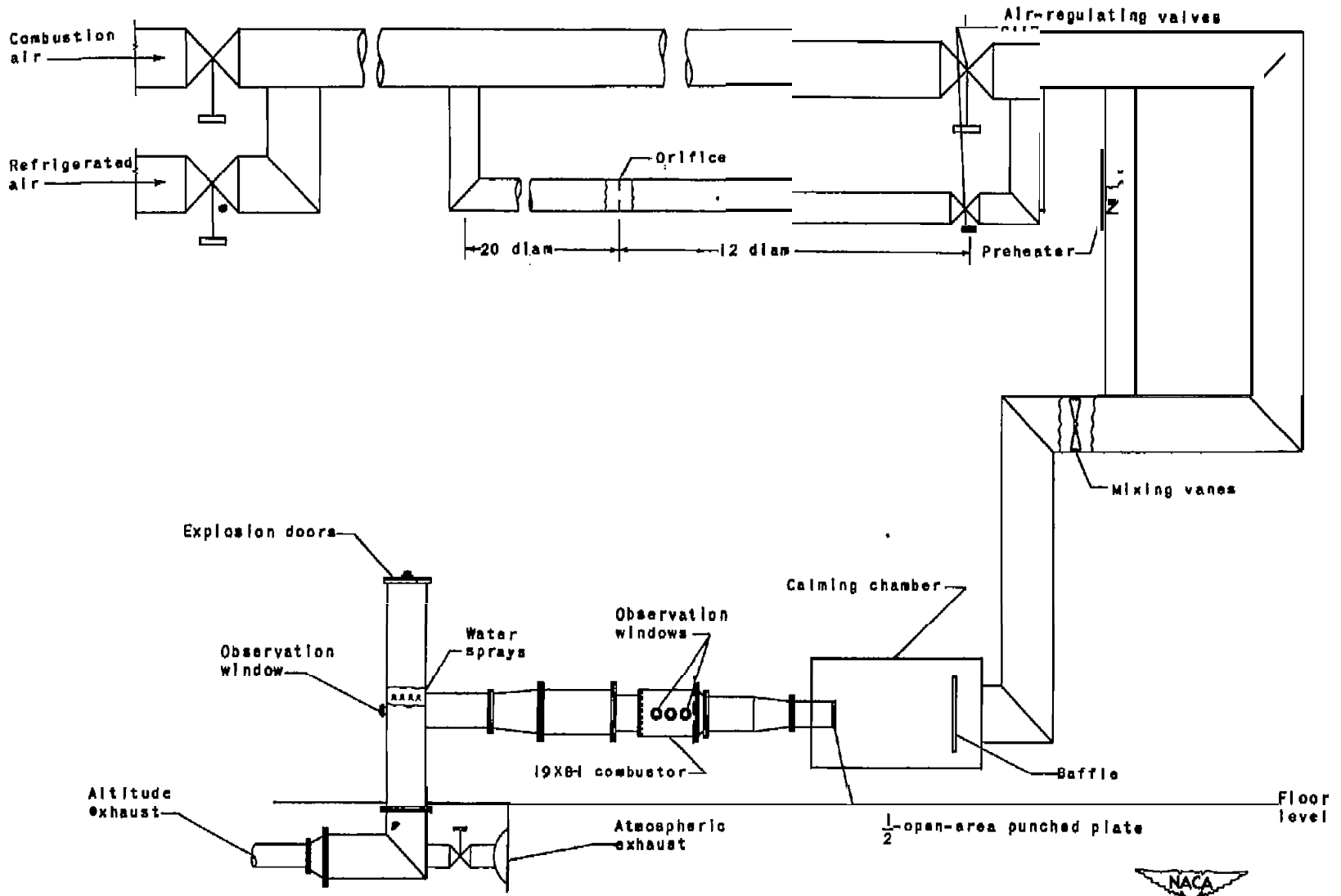


Figure 2. - Diagrammatic sketch of apparatus and installation of combustor for 19XB-1 turbojet engine.

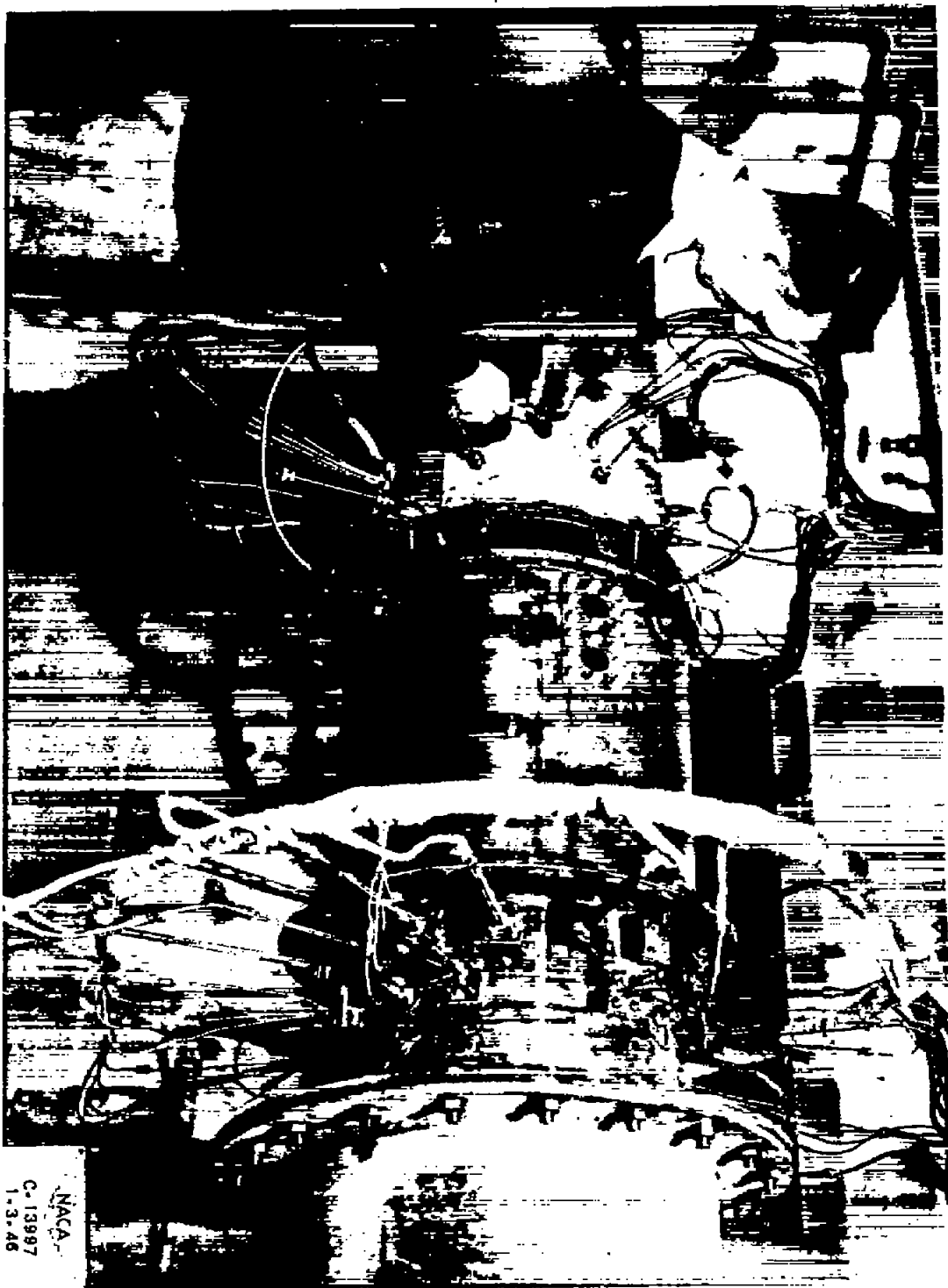


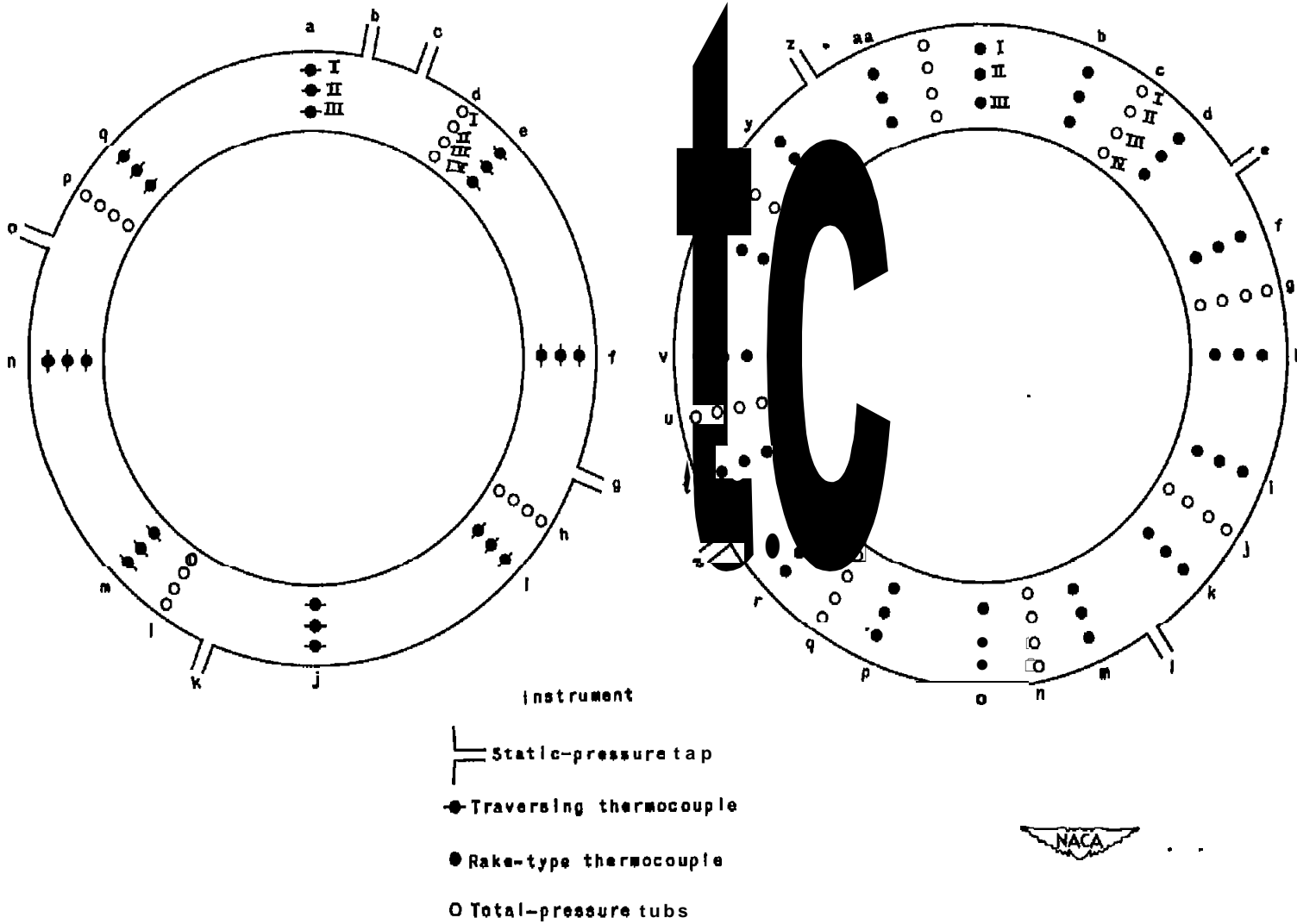
Figure 3. - Side view of installation of combustor for 9XB-1 turbojet engine.

NACA
C-13997
1-3-46

• -

• -

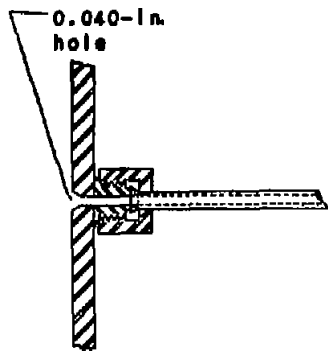
• -



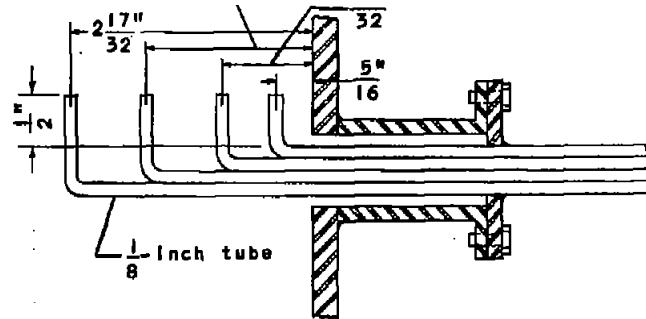
(a) Instrumentation plane 2 .

(b) Instrumentation planes 3 .

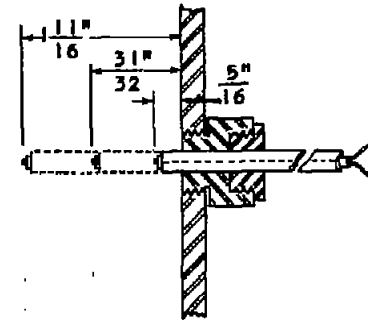
Figure 4. - Measurement stations at instrumentation planes shown in figure 1.



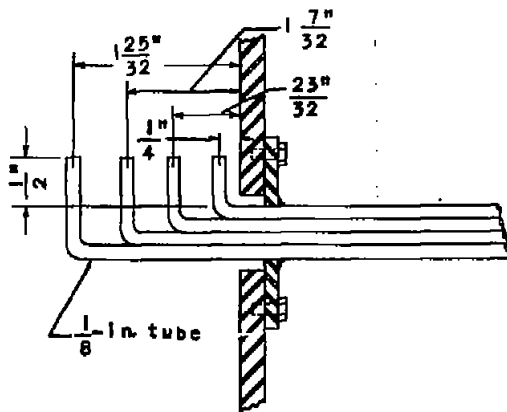
Static-pressure tap
used at instrumentation
planes 2 and 3



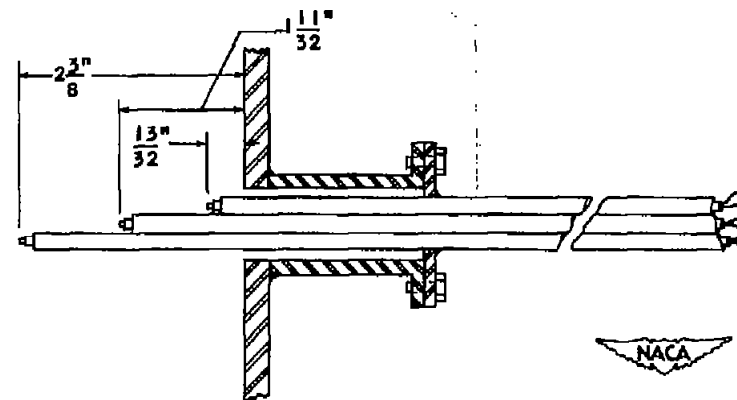
Total-pressure rake used
at instrumentation planes 3



Traversing thermocouple (iron-constantan)
used at instrumentation plane 2



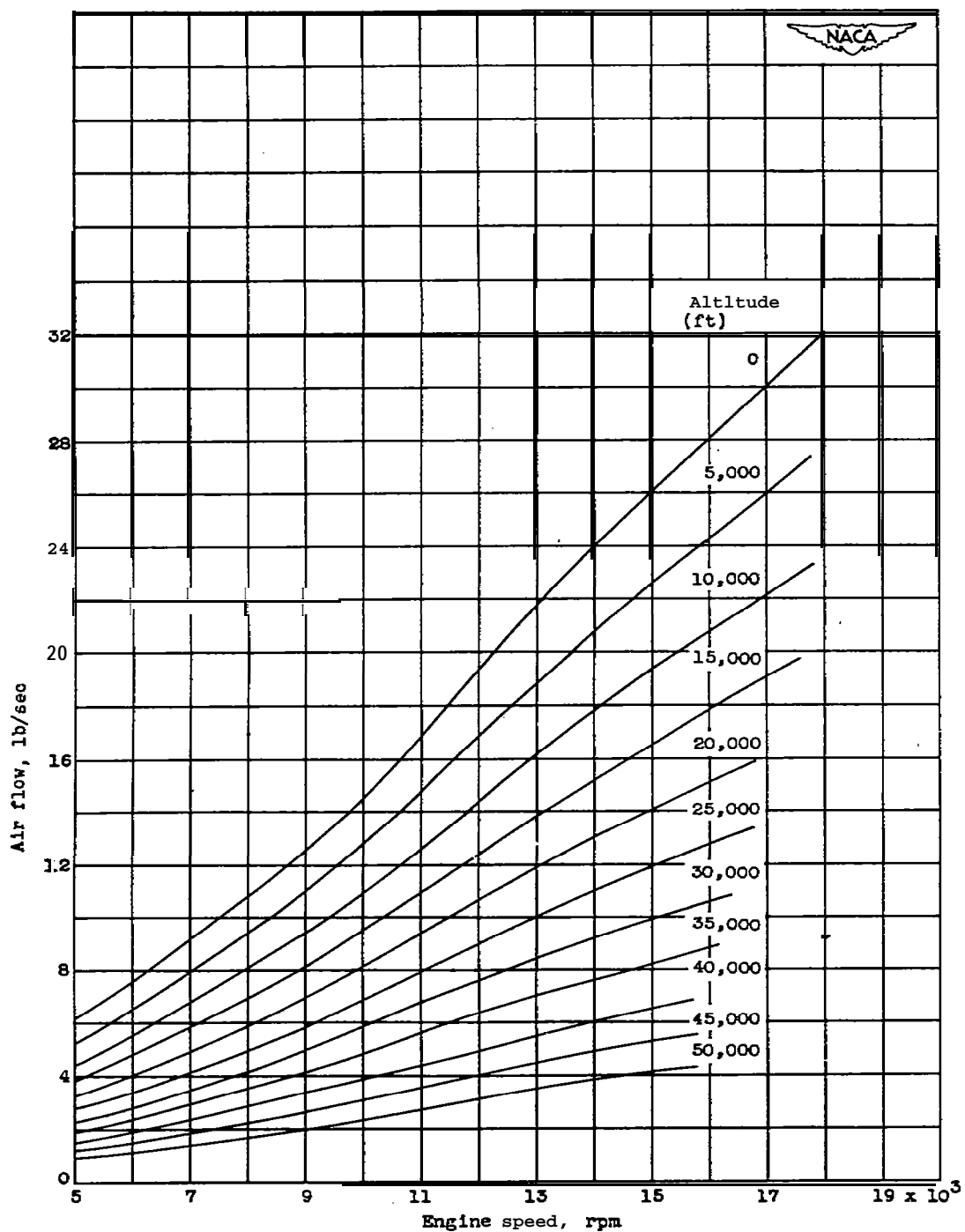
Total-pressure rake used
at instrumentation plane 2



Rake-type bare thermocouple (chromel-alumel)
used at instrumentation plane 3

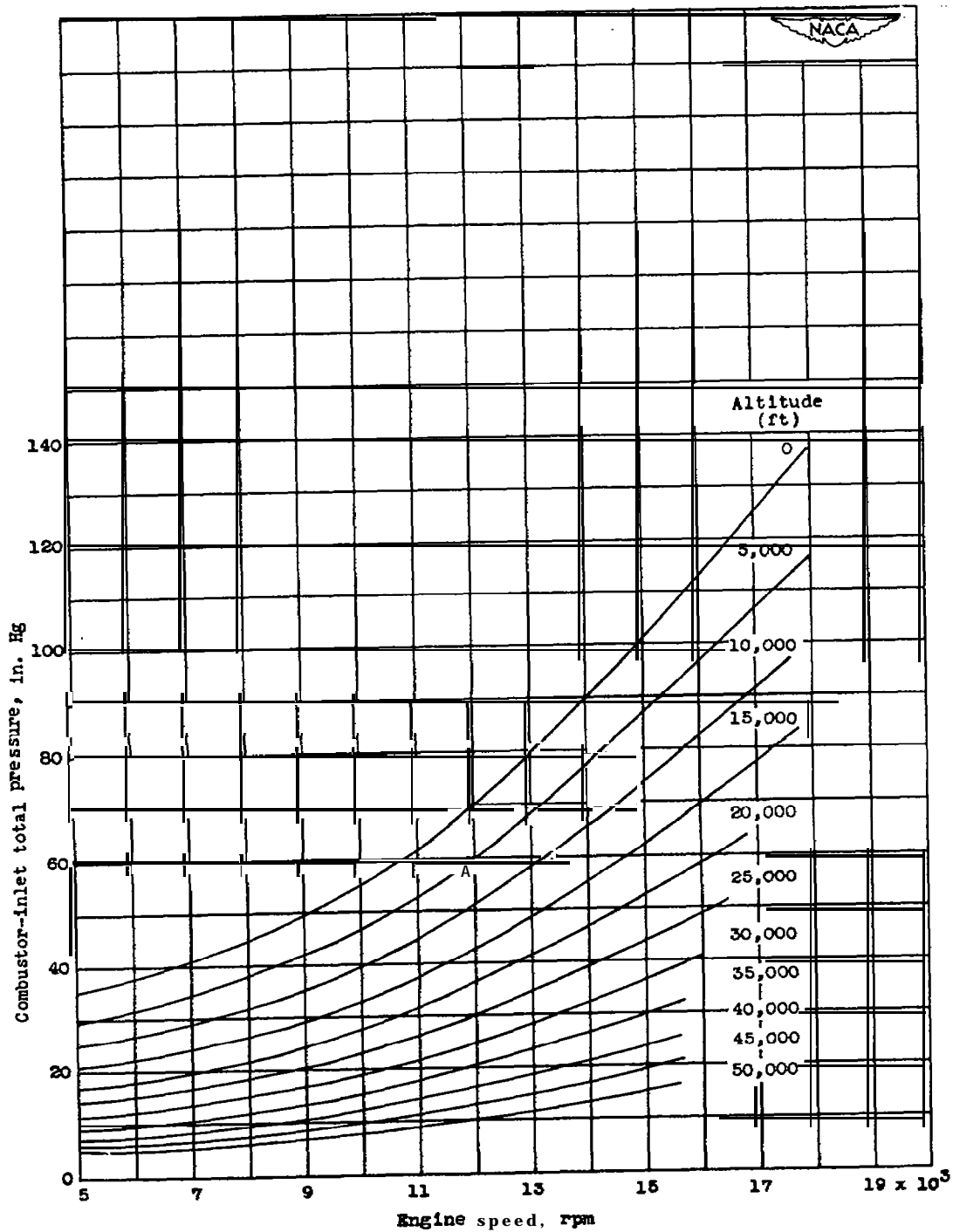


Figure 5. - Detail of temperature- and pressure-measuring instruments used at instrumentation planes shown in figure 1.



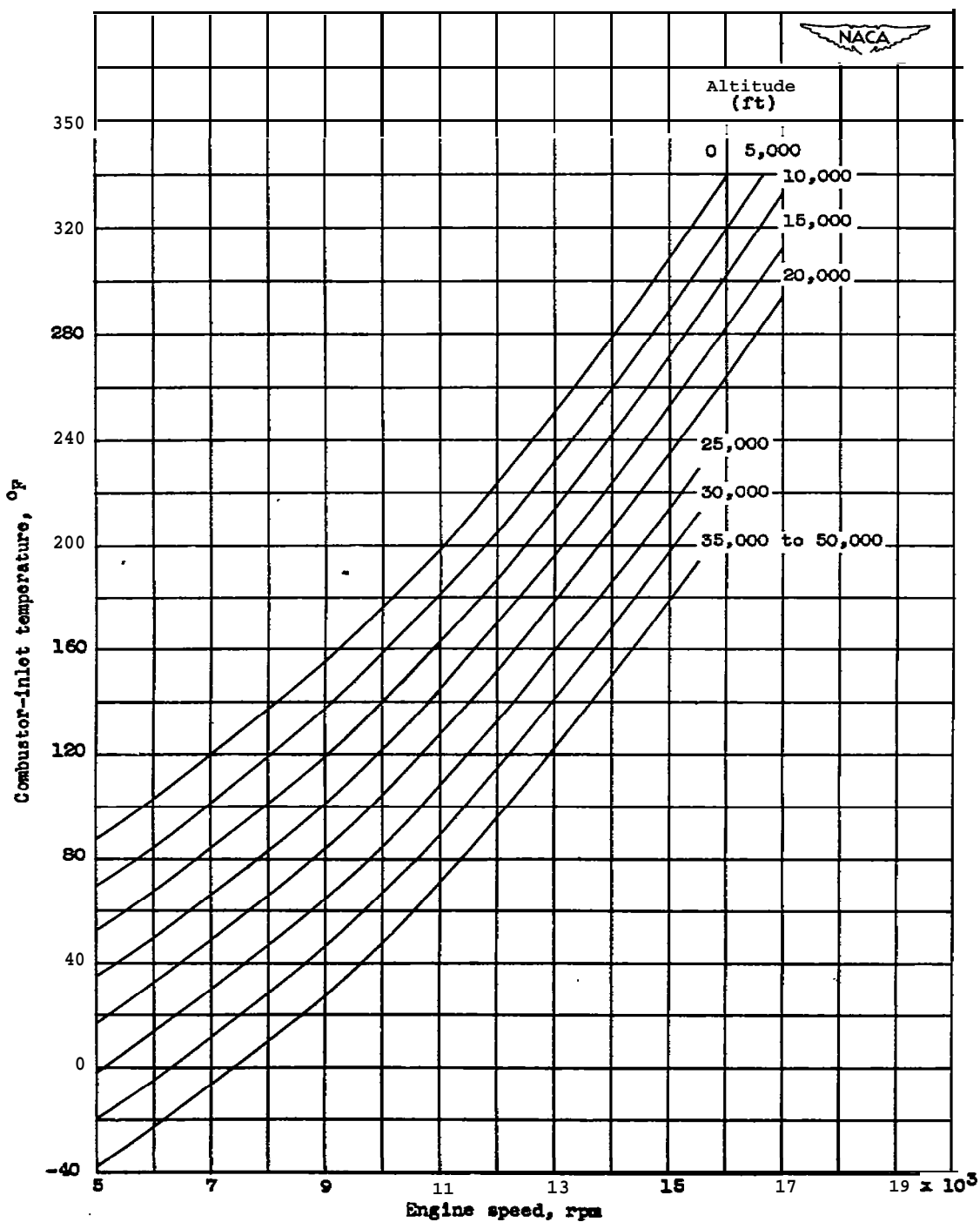
(a) Air flow.

Figure 6. - Estimated zero-mm performance characteristics of 19XB-1 turbojet engine. (Data from manufacturer.1)



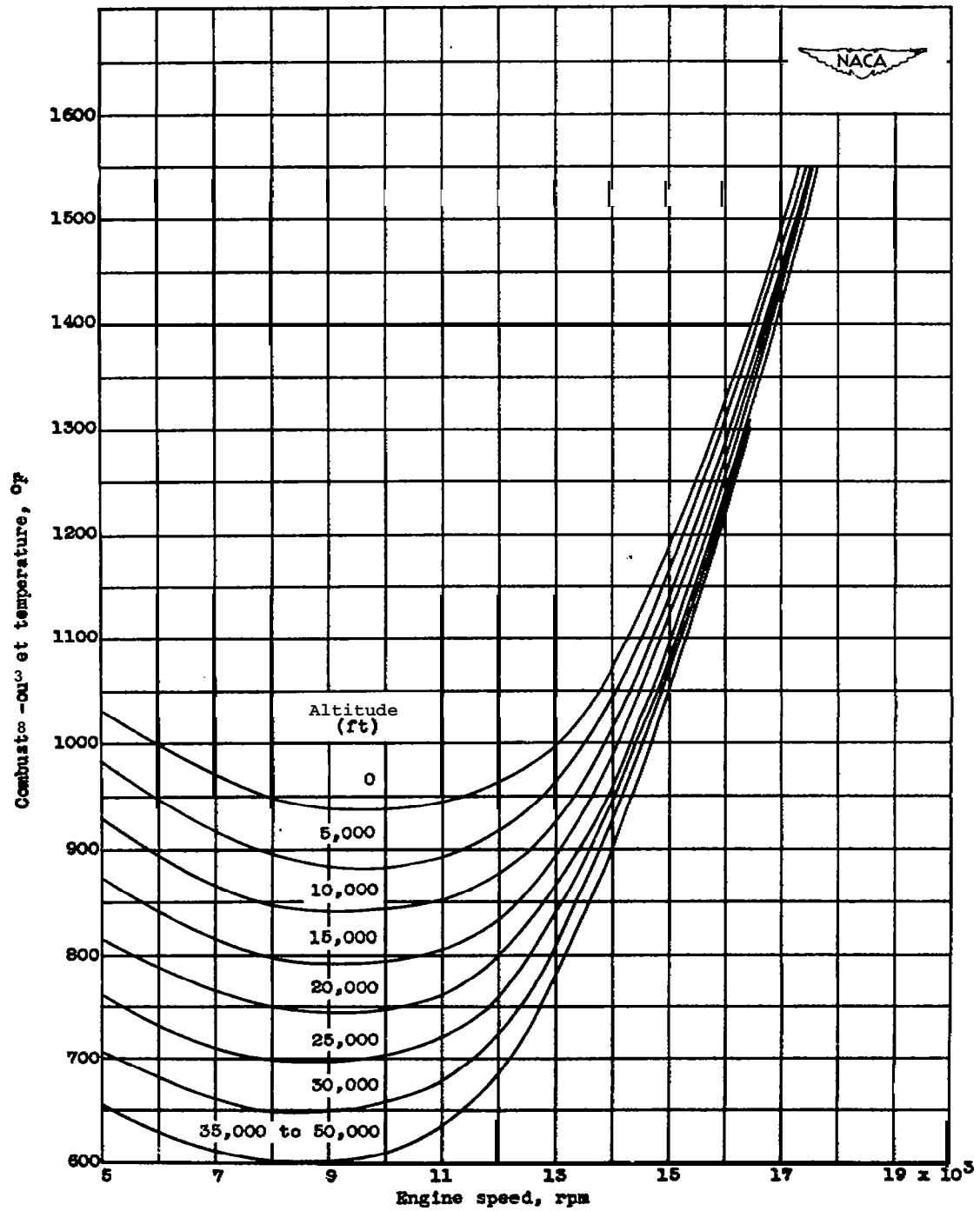
(b) Combustor-inlet total pressure.

Figure 6. - Continued. Estimated zero-ram performance characteristics of 19XB-1 turbojet engine. (Data from manufacturer.)



(c) Combustor-inlet temperature.

Figure 6. - Continued. Estimated zero-ram performance characteristics of 19XB-1 turbojet engine. (Data from manufacturer.)



(d) Required combustor-outlet temperature.

Figure 6. - Concluded. Estimated zero-ram performance characteristics of 19XB-1 turbojet engine. (Data from manufacturer.)

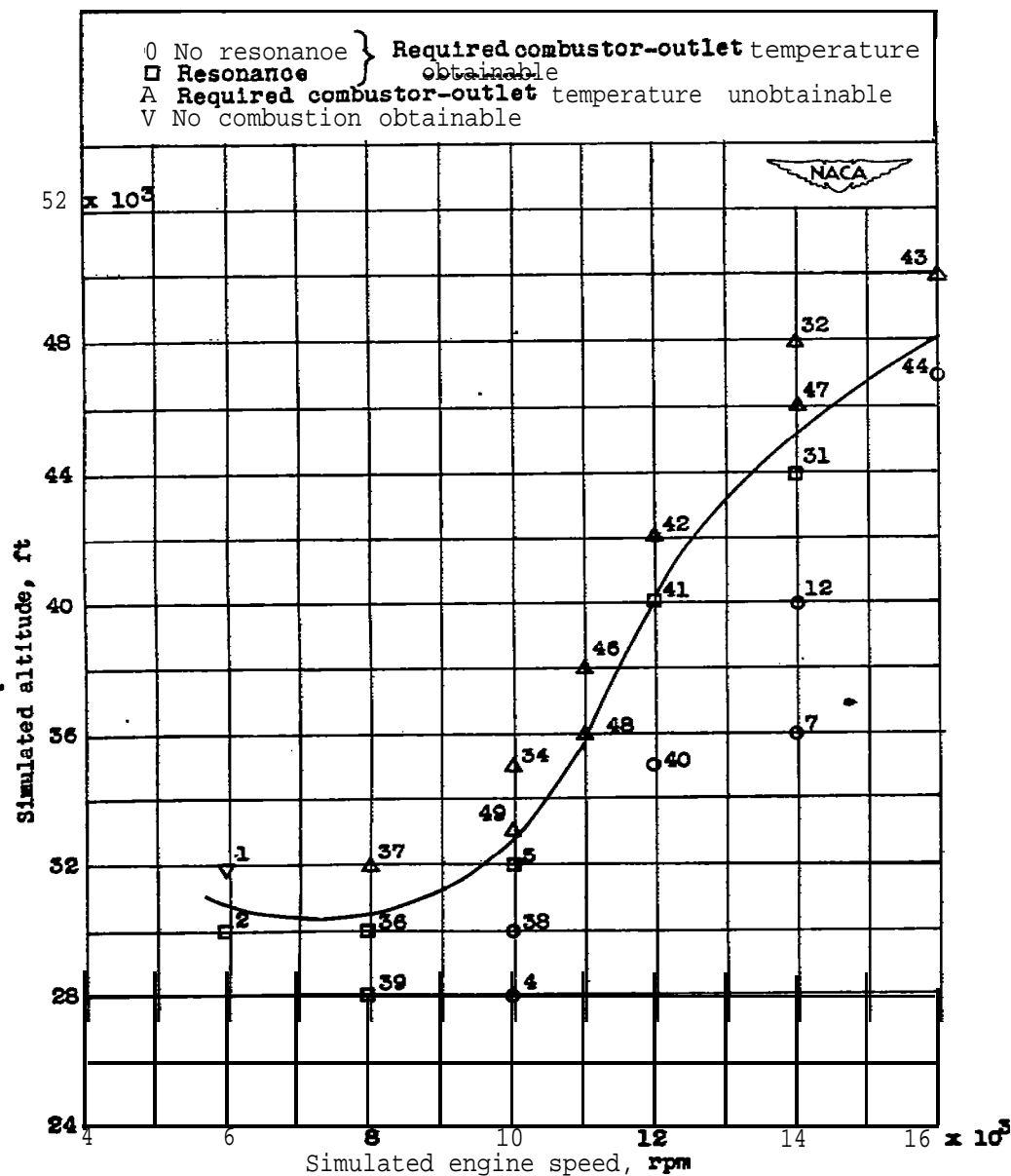


Figure 7. - Altitude operational limits of 19XB-1 turbojet engine as determined by performance of the combustor at various simulated flight conditions. Zero ram; fuel, AN-F-28, Amendment-3. Numbers designate points in table I.

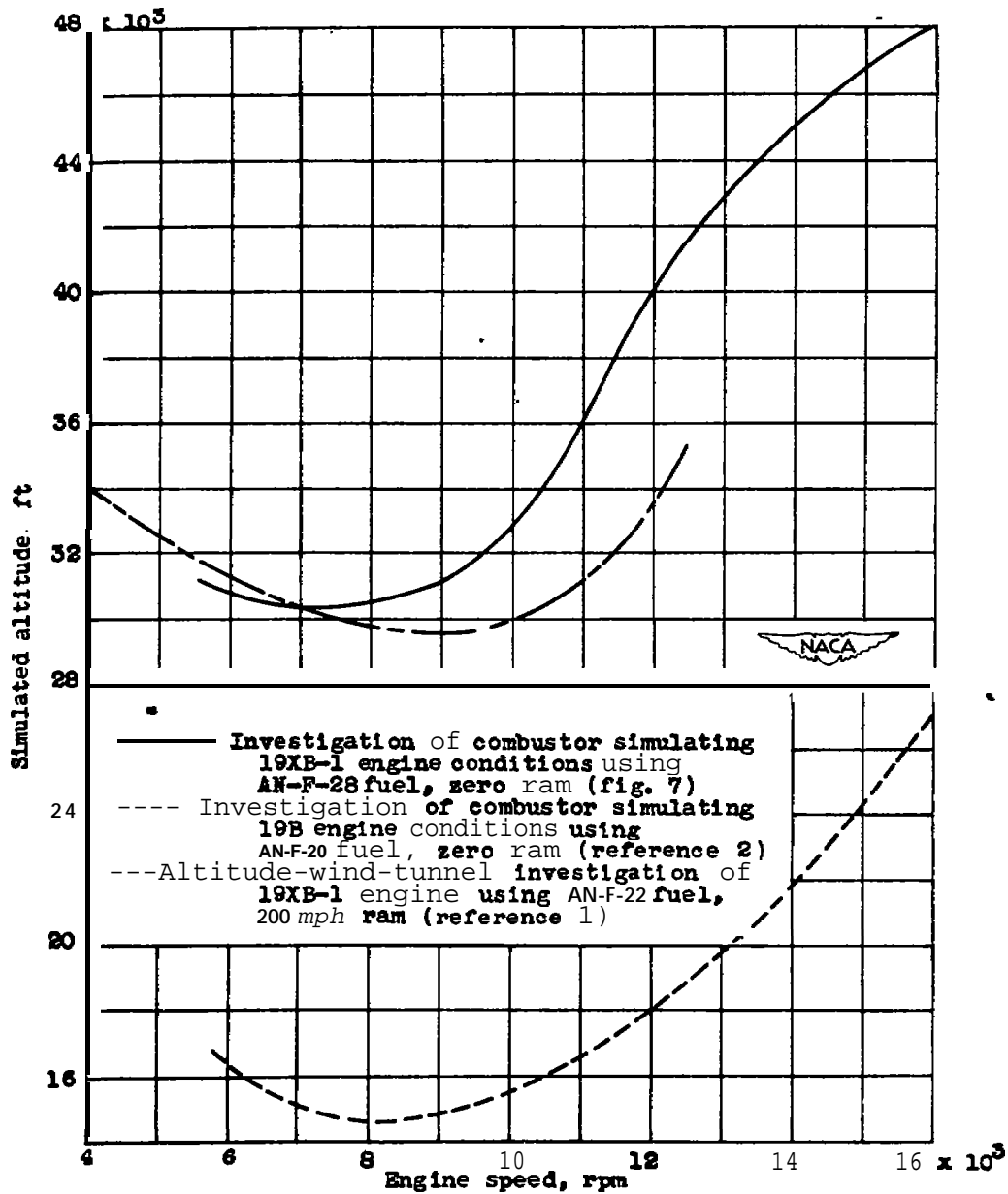


Figure 8 . Comparison of altitude operational limits of 19-inch turbojet engines as determined by 19XB-1 engine investigations and combustor investigations at both 19B and 19XB-1 engine conditions.

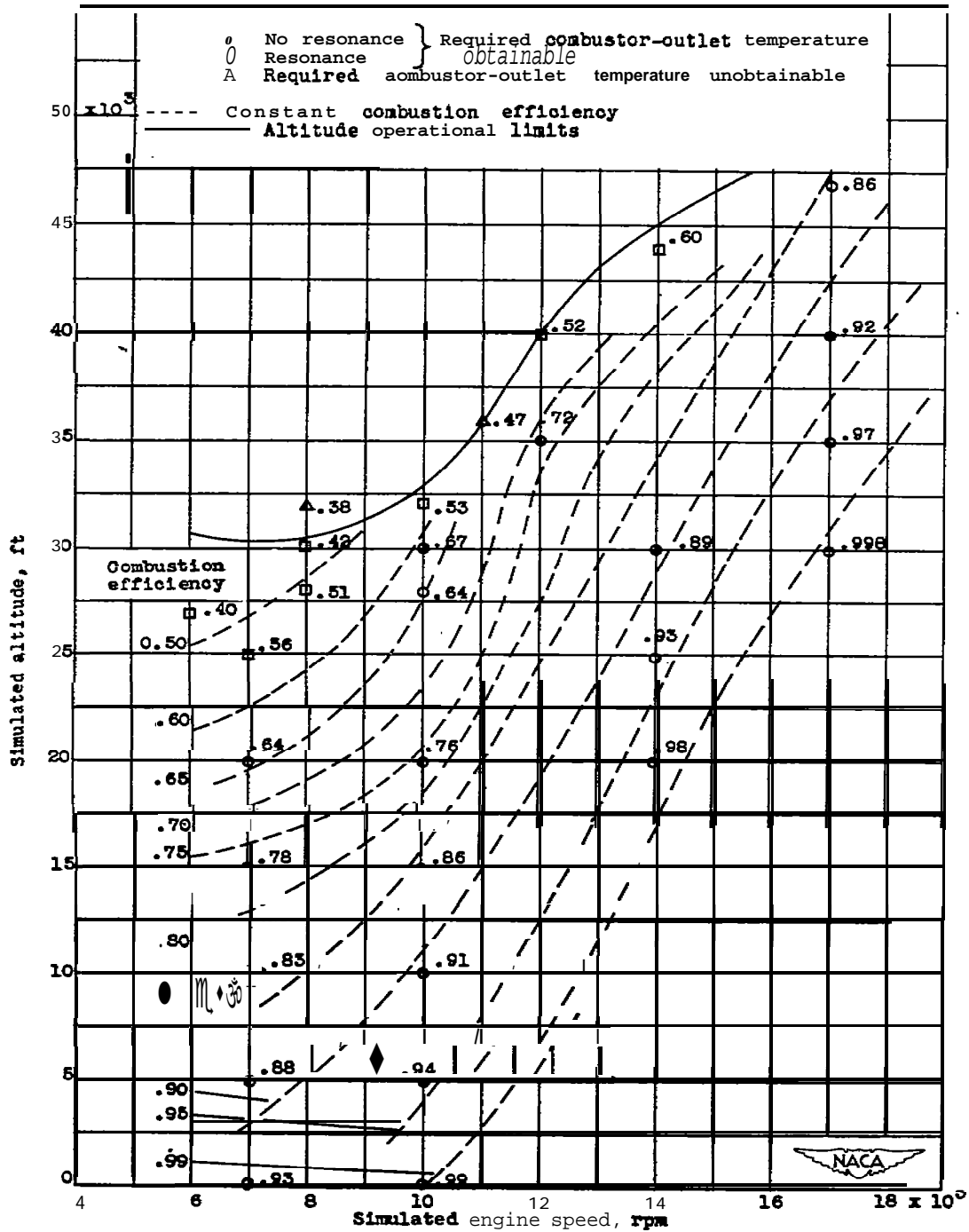


Figure 9. - Combustion efficiencies of combustor of 19XB-1 turbojet engine at various simulated flight conditions. Zero ram.

094

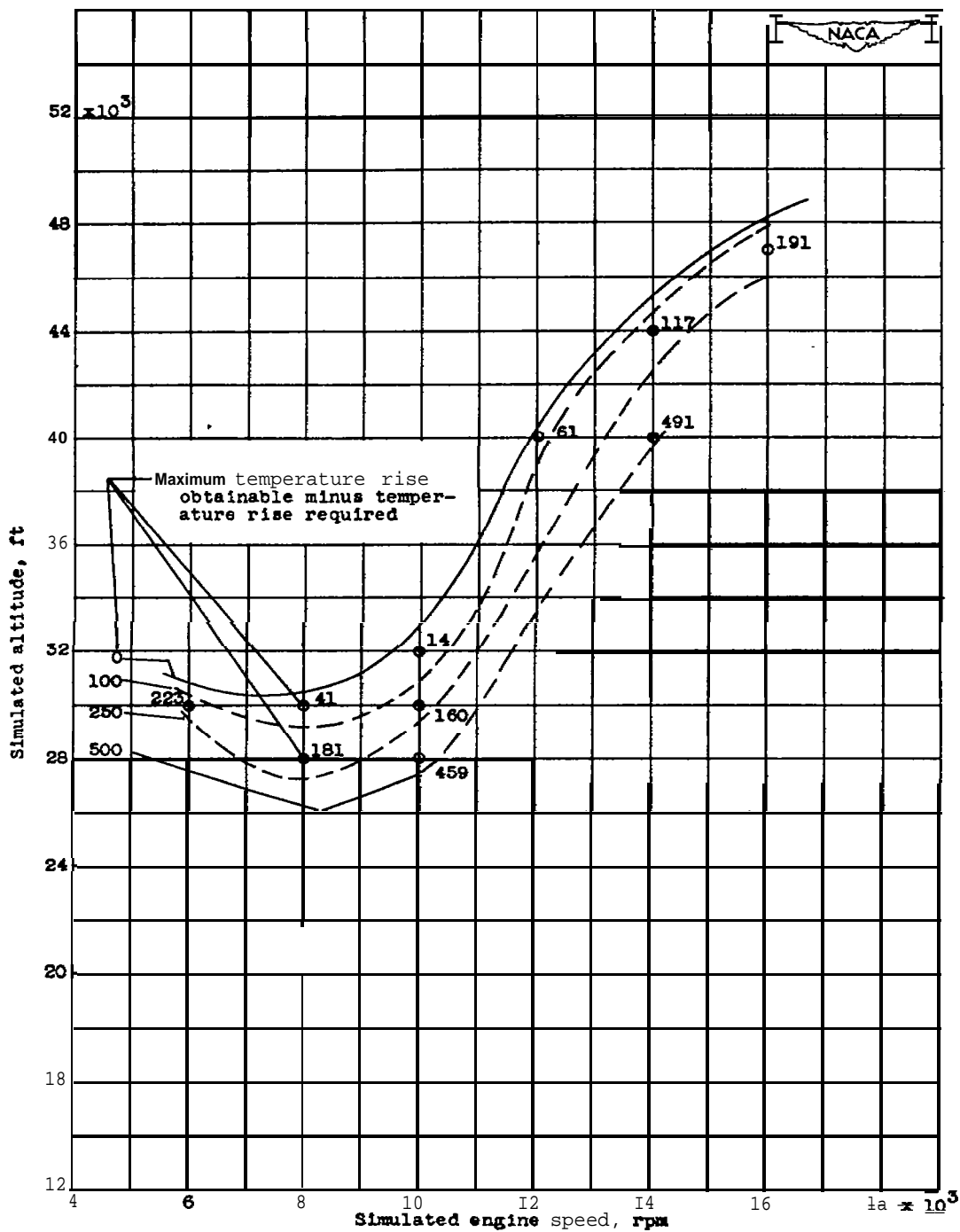


Figure 10. - Available acceleration of 19XB-1 turbojet engine as indicated by difference between maximum temperature rise obtainable in investigation of combustor and temperature rise required for nonaccelerating engine operation.

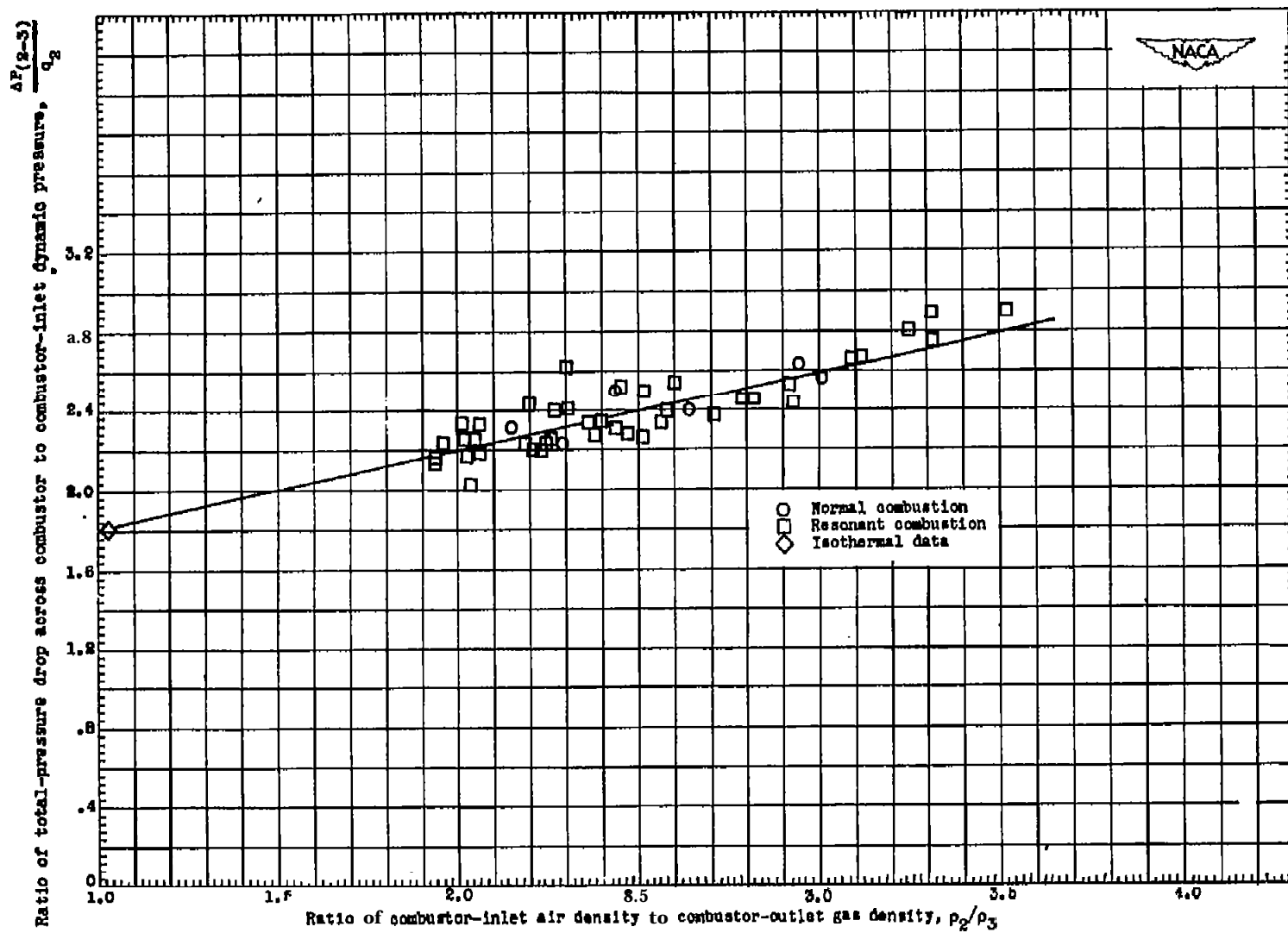


Figure 11. - Total-pressure drop across combustor of 19XB-1 turbojet engine, expressed as fraction of inlet dynamic pressure and as function of density ratio ρ_2/ρ_3 combustor.

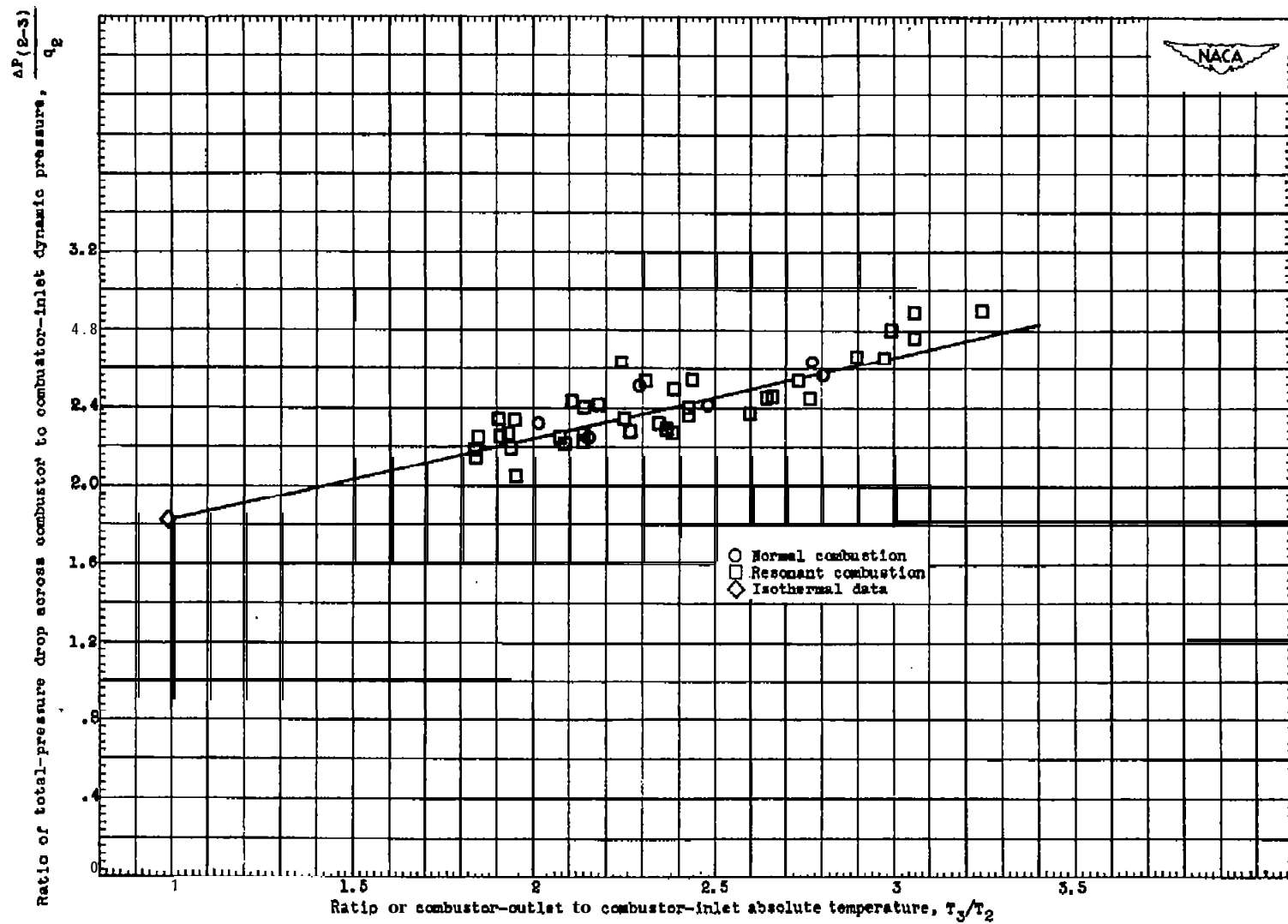


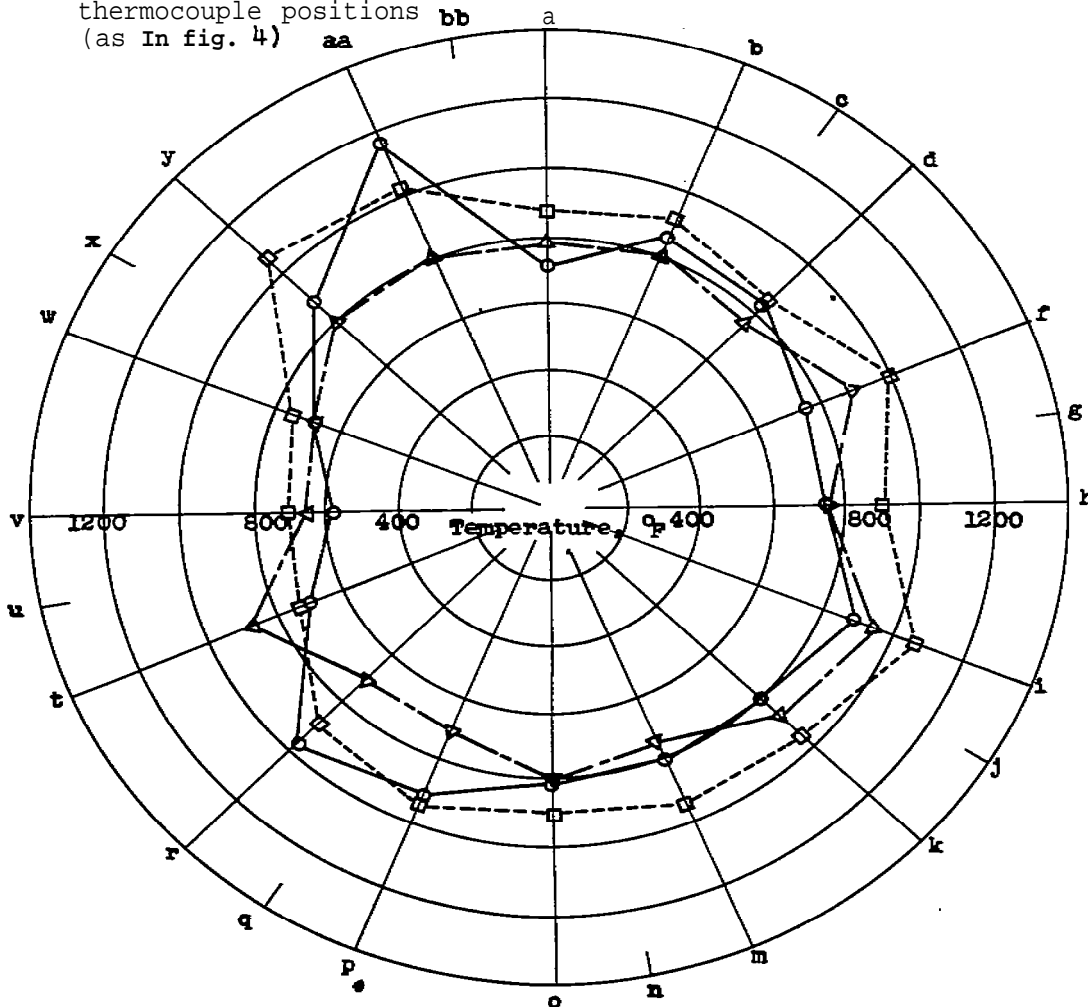
Figure 12. - Total-pressure drop across combustor of 19XB-1 turbojet engine, expressed as fraction of inlet dynamic pressure and as function of temperature ratio across combustor

Radial thermocouple positions



O I } Fig. 4
 □ II }
 Δ III }

a to aa Circumferential
 thermocouple positions
 (as in fig. 4) aa bb



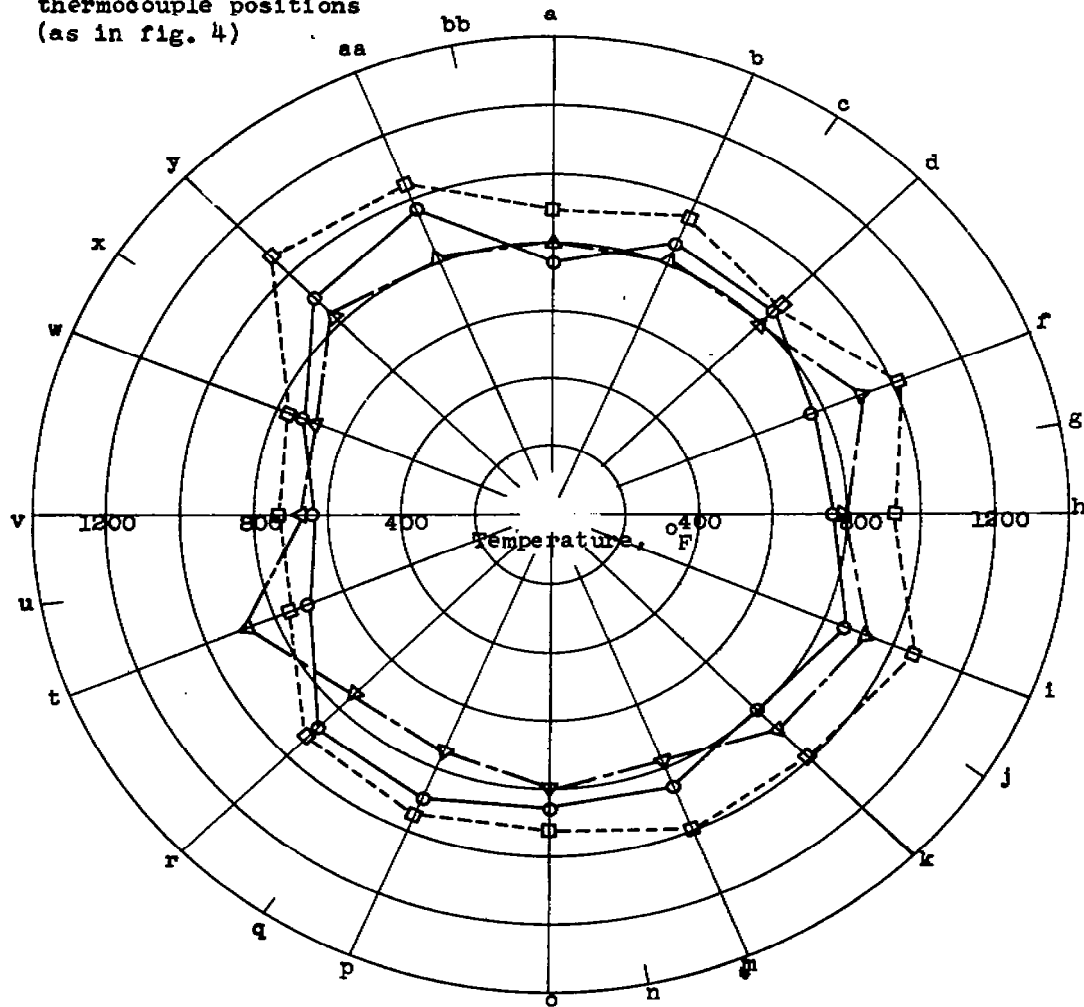
(a) Operating conditions simulating static engine operation at a rotational speed of 10,000rpm at an altitude of 15,000 feet.

Figure 15. - Temperature profiles at 19XB-1 combustor outlet.

Radial thermocouple
positions

○ I } Fig. 4
 □ II }
 △ III }

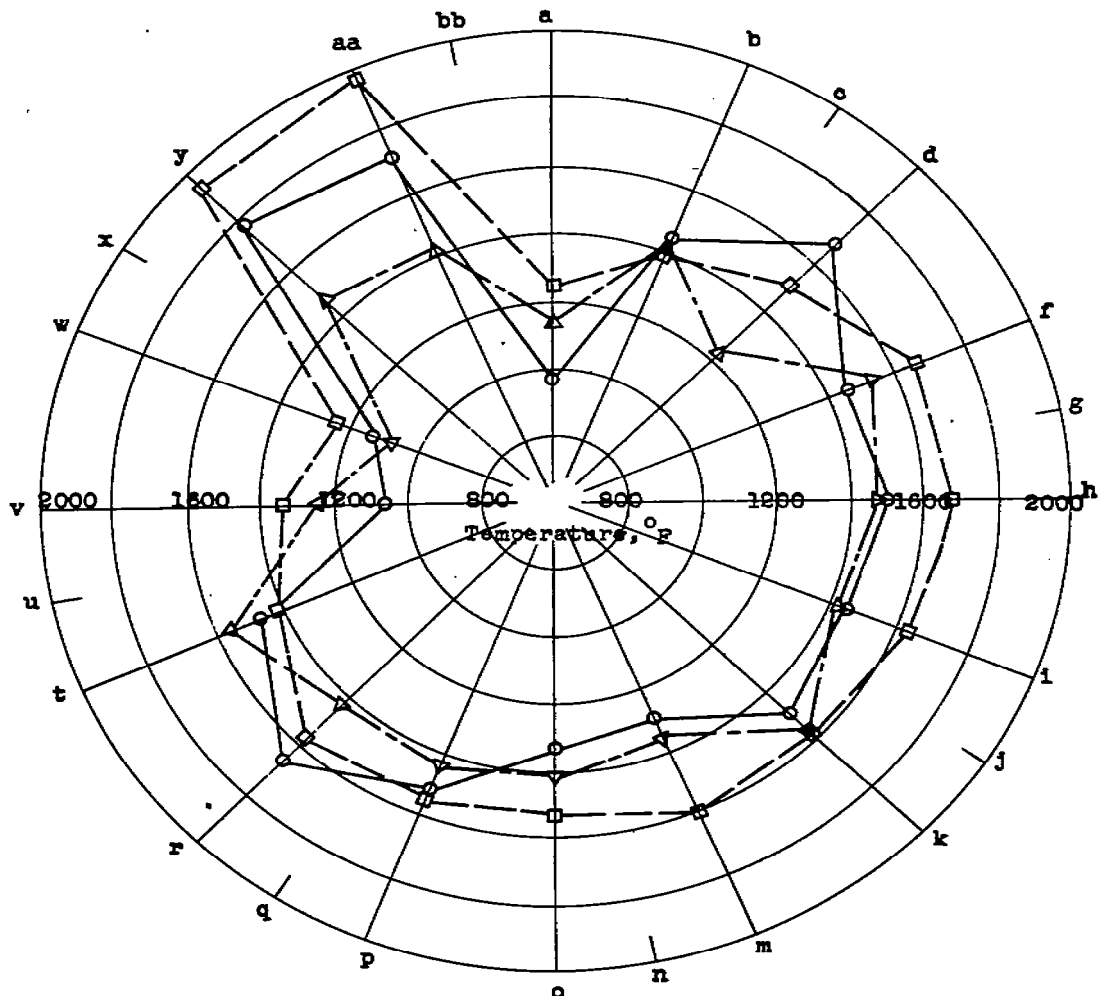
a to aa Circumferential
thermocouple positions
(as in fig. 4)



(b) Operating conditions simulating static engine operation at a rotational speed of 10,000 rpm at an altitude of 10,000 feet.

Figure 13. - Continued. Temperature profiles at 19XB-1 combustor outlet.

Radial thermocouple
positions
 0 I } Fig. 4
 □ II }
 Δ III }
 a to aa Circumferential
 thermocouple positions
 (as in fig. 4)



(c) operating conditions simulating static engine operation at a rotational speed of 17,000 rpm at an altitude of 47,000 feet.

Figure 13. - Concluded. Temperature profiles at 19XB-1 combustor outlet.

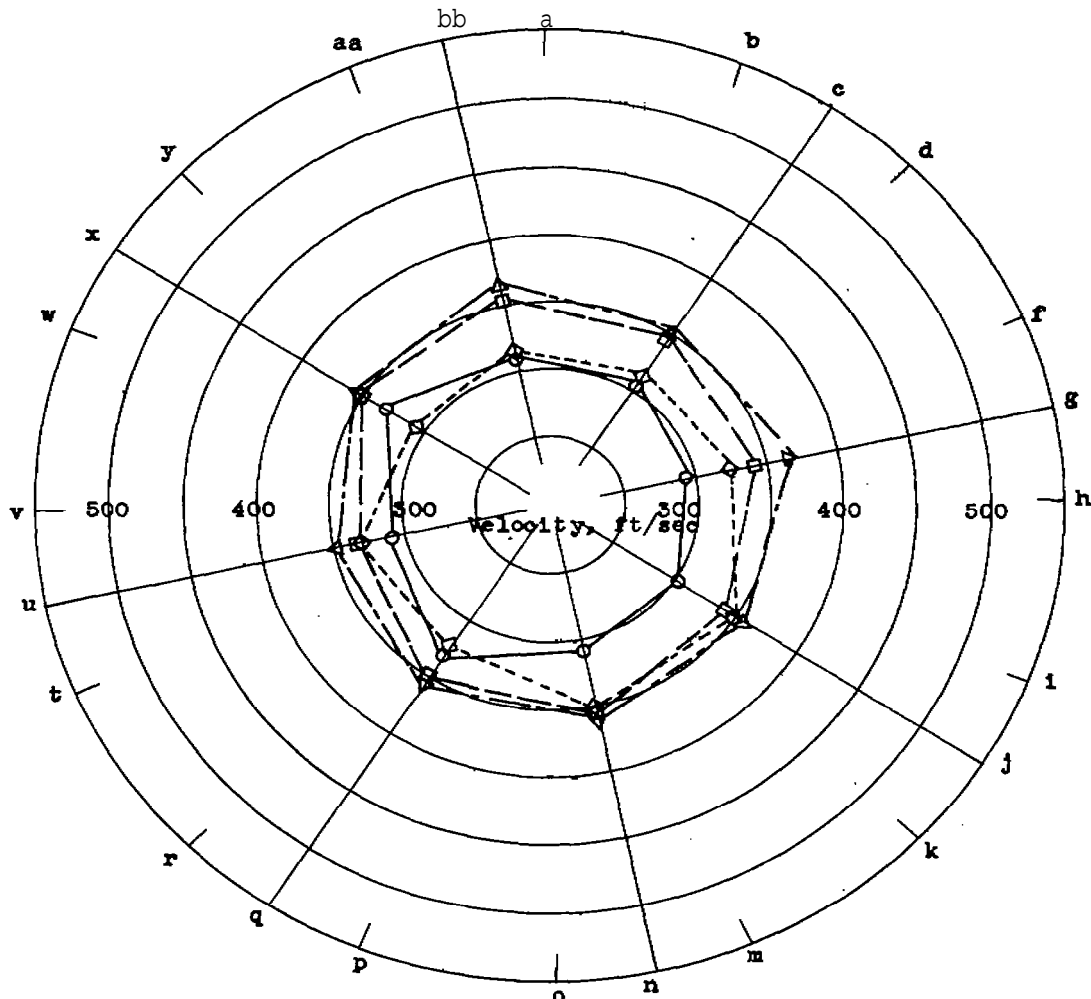
694

Radial **total-pressure** tap positions

0 I
 □ II
 △ III
 ◇ IV

Fig. 4

c to bb **Circumferential** total-pressure tap positions (as in rig. 4)



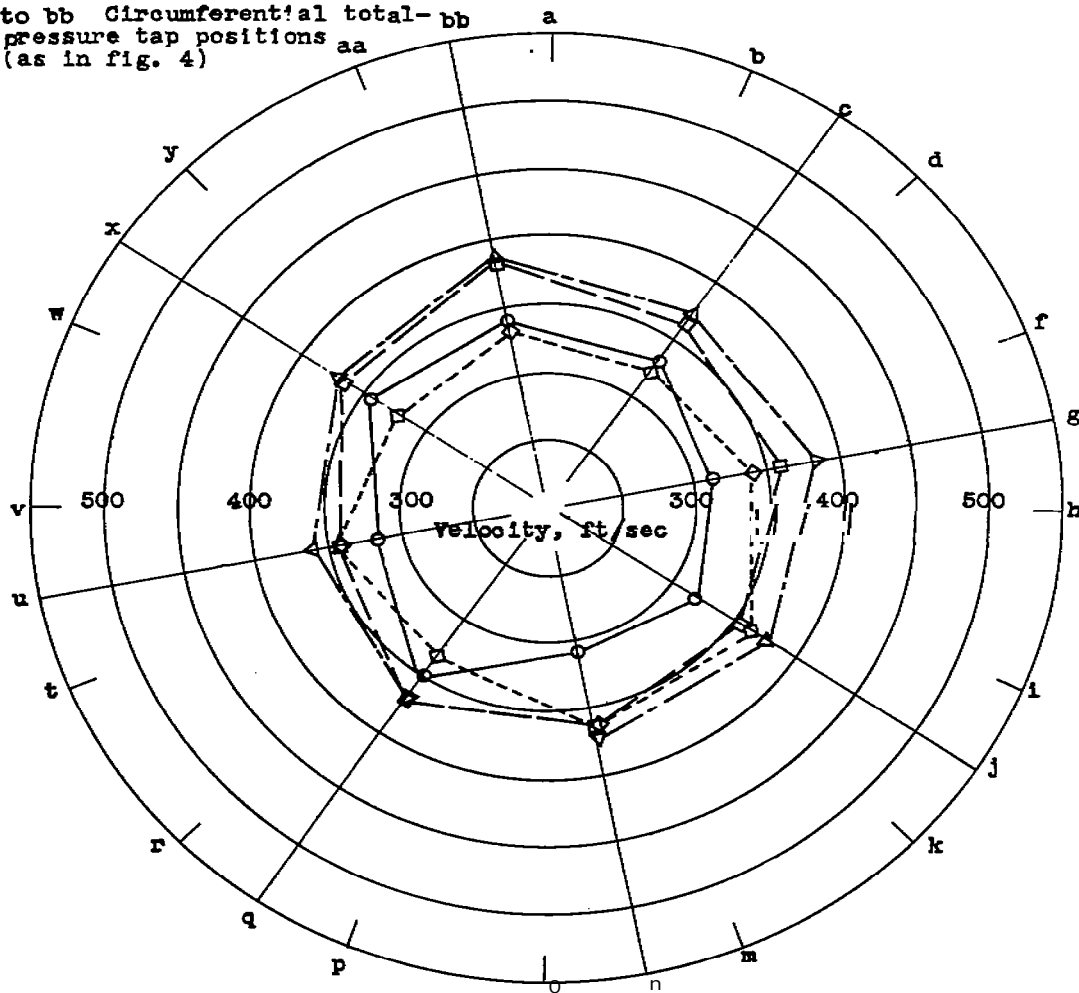
(a) Operating conditions simulating static **engine** operation at a rotational speed of 10,000 rpm at an altitude of 15,000 feet.

Figure 14. - Velocity profiles at 19XB-1 combustor outlet.

Radial total-pressure tap positions

○ I } Fig. 4
 □ II }
 △ III }
 ◇ IV }

c to bb Circumferential total- bb
 pressure tap positions aa
 (as in fig. 4)



(b) Operating conditions simulating static engine operation at a rotational speed of 10,000 rpm at an altitude of 10,000 feet.

Figure 14. - Continued, Velocity profiles at 19XB-1 combustor outlet,

694

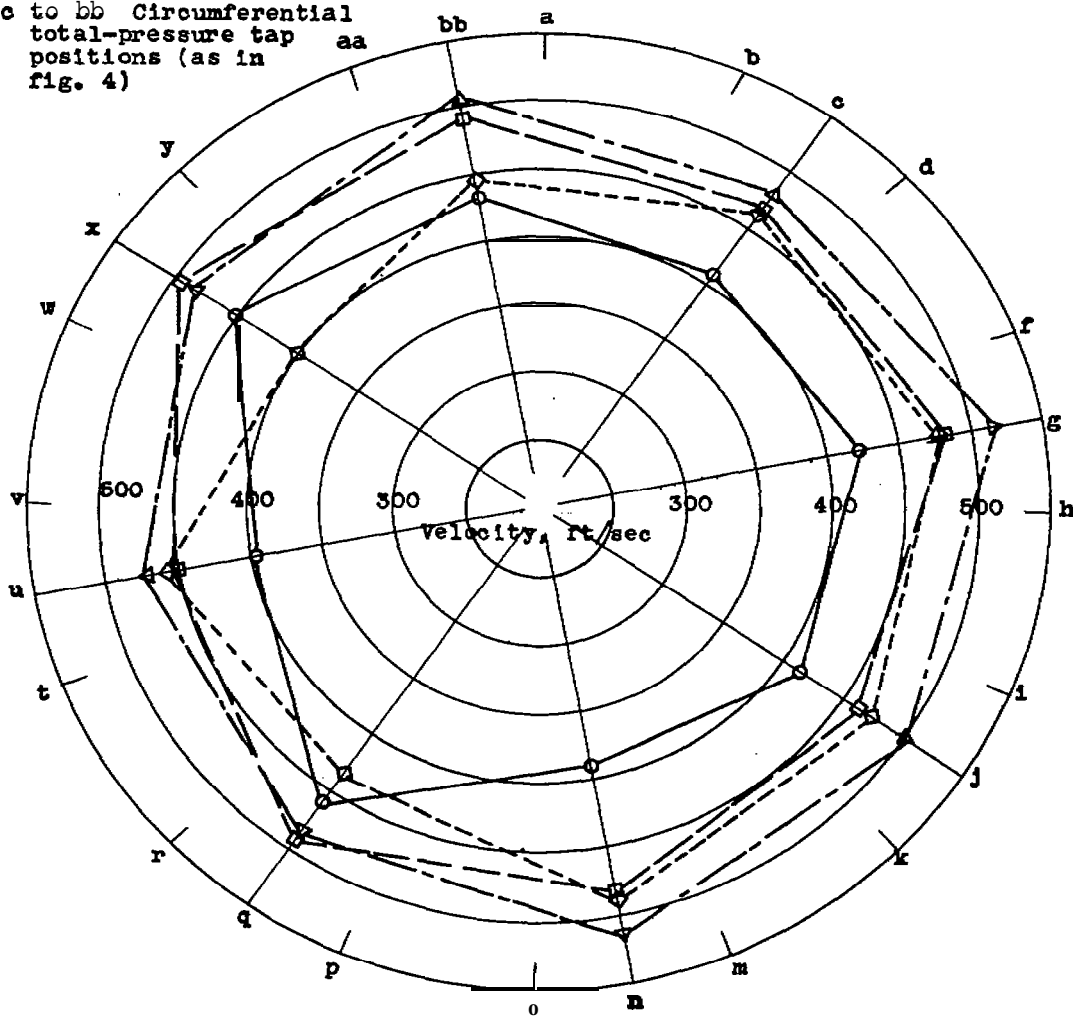
Radial total-pressure tap positions



○ I
 □ II
 △ III
 ◇ IV

Fig. 4

c to bb Circumferential total-pressure tap positions (as in fig. 4)



(c) Operating conditions simulating static engine operation at a rotational speed of 17,000 rpm at an altitude of 47,000 feet.

Figure 14. - Concluded. Velocity profiles at 19XB-1 combustor outlet.

694

NASA Technical Library



3 1176 01435 0632